# Woods Hole Oceanographic Institution

1930

# Biological/Physical Modeling of Upper Ocean Processes

by

Cabell S. Davis and John H. Steele

September 1994

## Technical Report

19950104 042

WHOI-94-32
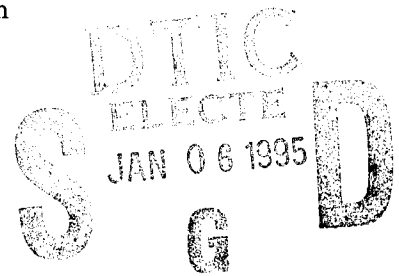
# Biological/Physical Modeling of Upper Ocean Processes

by

Cabell S. Davis and John H. Steele

Woods Hole Oceanographic Institution
Woods Hole, Massachusetts 02543
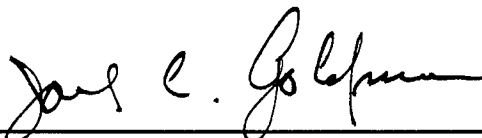
September 1994

**Technical Report**

Approved for public release; distribution unlimited.

**Approved for Distribution:**

Joel C. Goldman, Chair
Department of Biology

| Accesion For | | |
|---|---|---|
| NTIS CRA&I | | ☒ |
| DTIC TAB | | ☐ |
| Unannounced | | ☐ |
| Justification | | |
| By | | |
| Distribution / | | |
| Availability Codes | | |
| Dist | Avail and / or Special | |
| A-1 | | |

# WORKSHOP REPORT:

# BIOLOGICAL/PHYSICAL MODELING OF UPPER OCEAN PROCESSES

**Date:** June 7–12, 1993

**Location:** Woods Hole Oceanographic Institution (WHOI), Woods Hole, MA

**Conveners:** Cabell S. Davis and John H. Steele

# Table of Contents

## 1. Introduction

In order to increase communication between investigators who are modeling upper ocean biological/physical processes, a workshop was convened in Woods Hole on June 7-12, 1993 (see Appendix I for names and addresses of participants). This workshop was part of our on-going URIP project entitled "Modeling Biological-Physical Interactions: A Population Biological Approach" sponsored by ONR (Grant N00014-92-J-1527). The two principal goals of the workshop were to: 1) identify critical problems related to mixed-layer biological-physical models, and 2) develop approaches for solving these problems.

The workshop was organized into two parts to address these goals. The first part, held over the first day and a half, included three overview presentations given in plenary followed by working groups, organized along disciplinary lines, to identify critical issues. The second part of the workshop consisted of working groups, organized across disciplines, using "hands-on" modeling to address critical aspects of coupled biological-physical models.

Overview presentations were given during the first morning to provide background information on physical mixed-layer models (Kenneth Denman), biological models with age-structured herbivore populations (John Steele), and microbial-loop dynamics (David Caron). Following these presentations, the working groups were organized to address problems associated with 1) physical modeling, 2) structured herbivore vs bulk nutrient-phytoplankton-zooplankton models, 3) food-web models, and 4) coupling complex biology to 2- and 3-D physical models.

After plenary reports of these first-format working groups, the second-format working groups were formed to begin modeling in the areas of 1) coupling simple food-web models to several different physical models, 2) development of NPZ models which include microbial-loop dynamics, and 3) development of structured-zooplankton models and incorporation into NPZ models.

An annotated bibliography of existing mixed-layer models was provided by David Archer and is given in Appendix II. Brief descriptions of three coupled biological/physical mixed layer models is given in Appendix III.

## 2. General Reviews–Critical Issues (from 1st-format Working Groups)

### 2.1 *Physics of Mixed Layers*

Archer, Chen, Denman, Doney, Gawarkiewcz (Rapporteur), Glover (Chair), Hood

- The biological questions which are being addressed should affect the choice of model being used.
- Models have clearly defined weaknesses which must be taken into consideration before use. For example, P-W-P assumes no vertical velocity shear is present in the mixed layer, while observations show such shear is frequently present.
- We should be thinking about upper ocean models in general (i.e. including the thermocline) rather than strictly limiting ourselves to calculating the "mixed layer depth". This is particularly important when considering heat flux divergences in 1-D models (what depth do you "advect" the heat away when modelling an annual cycle?). Lateral mixing processes may be important in the thermocline in distributing nutrients

along isopycnals. The vertical transport of nutrients into the base of the mixed layer needs to be considered.

- Observations of Jenkins clearly show an enhanced vertical flux of nutrients into the euphotic zones which current models using standard parameterizations cannot explain. Is this due to mesoscale variability and eddy pumping? What should be done with 1-D parameterizations if mesoscale effects are important?

- What role do large and small-scale fronts play in understanding mixed layer dynamics? How important are horizontal inhomogeneities in understanding the performance of 1-D models when compared with time series of observations? How should mixing within frontal zones be parameterized? More observations with good horizontal resolution will be necessary to make progress in this area.

- What level of complexity is needed in prescribing optical fields? Under what conditions do the absorption characteristics affect the temperature distributions in the vertical?

- There are major questions regarding the Lagrangian descriptions of flow fields in the upper ocean. In particular, the Lagrangian behavior of particles in fields where the mixing coefficients are changing with depth is not well understood. Good Lagrangian information is necessary to describe light histories of particles as well as predator-prey contact rates.

- How will the use of Large Eddy Simulations affect our understanding of the mixed layer? These models seem to give results that are very different from both P-W-P as well as Mellor-Yamada Level 2.5.

- The integration of data from various acoustic observational techniques which resolve the turbulent eddies in the mixed layer should lead to much better parameterizations of the characteristics of the turbulence. Hopefully, this will occur over the next 5 years or so.

- In the coastal regions, the interaction of the bottom and surface boundary layers is not well understood. Much more work in the future will be necessary to resolve this issue.

- Surface forcing in regions in which no buoy data is available is a major problem. Wind products tend to severely underestimate maximum wind velocities, which leads to major differences in surface fluxes.

- Processes associated with the surface wave field are not included in most present day mixed layer models. The effects of Langmuir cells and wave dissipation on the turbulence fields will have to be addressed in the future.

*Conclusions*
- Horizontal variability is not well known.
- Lagrangian nature of flows are not well known.
- Acoustic observational techniques will help resolve turbulence fields.

2.2 *NPZ vs NP-(Structured-Z)*

Armstrong, Bollens, Caswell (Chair), Frost, Lewis (Rapporteur), Steele

- Why structure only herbivore populations?

2

- No reason, in fact the group decided in many cases that structure could be required in a number of different trophic levels.
- What is the purpose of structure?
    - This was one of the primary questions that came around, as it is possible to add structure to a wide variety of populations and trophic levels while accomplishing nothing more than tying up your computer. Applications in which stage-structured models may be needed include:
    - Fisheries models in which it is necessary to know the abundance of a wide variety of zooplankton species; prey for the larval fish.
    - Data comparison and validation. However, the converse of this is that there is little point in running a stage structured model where you have no information concerning the population structure.
    - For comparison to NPZ models to determine whether the introduction of stage structure has a significant effect on the dynamics.
    - To introduce stage specific behavior.
    - To represent the microbial loop and other multispecies models.
    - Time scales of response by a species with a long growth period may require stage structure to be adequately represented.
    - Abundances may respond with a periodicity determined by the generation times.
- Problems with such stage models include:
    - You may need multiple phytoplankton populations to support a multi- species grazing population.
    - Truncation of the trophic models to the highest trophic level of relevance.
- Vertical structure:
    - Need the physical dynamics to transport plankton, but you may not need a full one-D biological model to couple to the physics.
    - Behavioral effects.
- Incorporation of physical models.
    - May not need full resolution of PWP model.
    - Should explore sensitivity of models to increased physical complexity.
- Suggestions:
    - Use output of physical model to drive biology: use temperature and diffusivity values, time-smoothed
    - Time smooth and space smooth spatial model at varying scales to determine what effect the reduced complexity will have on the biology.
        - Use 100 point PWP results on 100,50,20, etc. level biological model.
        - Use time averaged PWP fields, determine effect of high frequency activity.
    - Combine the organisms of Caron's work with the model written by Armstrong.

### 2.3 *Food web models and validation with data*

Caron, Landry (Chair), Landsteiner (Rapporteur), Moisan, Sarmiento
- Critical Task:
    - Implementation of food-web models with appropriate microbial community structure and interactions.

3

- Minimal structure of a microbial loop model:
  - Three phytoplankton (pico, nano, and micro)
  - Heterotrophic bacteria
  - Two levels of protozoan consumers (nano and micro)
  - DOM flows from phytoplankton excretion, sloppy feeding, decay of protozoan feces, and mortality.
- Relevance of microbial dynamics in food webs: - Basic structure of lower trophic levels in all upper ocean environments.
  - Allows partitioning of primary production among size classes, a major distinguishing characteristic of different environments or seasons.
  - Essential to understanding the basic mechanisms of phytoplankton control (i.e., grazing vs nutrient limitation).
  - Provides a realistic resource environment for modeling of macro-consumers.
  - Provides a versatile format for other desirable model outputs:
    - new production ratio (recycling pathway)
    - multi-elemental cycling
    - vertical fluxes (sinking vs. non-sinking feces)
- Necessary and existing data:
  - standing stocks and elemental composition of all populations
  - size-fractionated primary production
  - protozoan grazing rates and behaviors
  - protozoan growth efficiencies
- Problems:
  - Thresholds
  - Closure through metazoans (multiple species and stage-structure)
  - Allometric relationships
  - Depth structure (controlled through light and nutrient kinetics)
  - Selective feeding on multiple-size classes

## 2.4 Problems in use of 1-D coupled biological/physical models

Davis, Flierl (Chair), Franks (Rapporteur), Levin, McGillicuddy, Olson

- Critical Issues
  - Horizontal advection necessary over long time-scales to balance deep heat flux, nutrient flux
  - Timescales of mixing in the model vs. biological rates - how to parameterize faster rates (e.g. photoadaptation) in mixed layers
  - How to parameterize patchiness and variability of biological fields
  - How does variance propagate trophically, temporally - can we use statistics of biological distributions as variables in the model?
  - When is use of PWP model appropriate?
    - short-term variation in seasonal thermocline; days-weeks
    - if coupled to "good" GCM, may be able to extend its usefulness

4

– need to consider importance of remnant layers to vertical fluxes over long times scales. May necessitate forced boundary conditions, or coupling to 2-D or 3-D PE model.

- Suggestions:
  - use a number of different models of the same physical/ biological problem (sensu Martin) to assess utility, and observe differences.
  - use large-eddy simulation models for more realistic 2-D or 3-D representation of smaller scales
  - use Deardorff-type model (4th order closure) rather than PWP

## 3. Reports of Work (2nd format Working Groups)

### 3.1 *Comparing mixed layer models containing simple plankton dynamics*

Chen, Denman (Chair), Doney, Flierl, Franks, Gawarkiewcz, Glover, Hood

### 3.1.1 *Goal*

To compare the behavior of several models of mixed layer physics coupled to simple Nutrient-Phytoplankton-Zooplankton-Detritus (NPZD) models.

### 3.1.2 *Physical Mixed layer models*

The group concentrated primarily on completing the comparison and coupling of mixed layer models to a simple NPZ model, all set up beforehand by Glenn Flierl. In addition S. Doney and D. Glover set up a mixed layer model being developed at NCAR with an NPZD model, and R. Hood explored the behavior of an NPZD model coupled to CONV and PWP (described below). The following mixed layer models were included in the comparison:

- CONV - This model was the simplest, consisting of a mixed layer depth of 10 m or else one determined by simple convective adjustment, whichever was deeper. Each day at noon, the mld retreated to 10 m and each night it reached a depth ranging from about 20 m in summer to 80 m for 1-2 months in the winter (which was the bottom of the model). The annual cycle was more realistic than in the plots to follow, which track the mld at midnight, several hours before the deepest mixing each night.
- PWP (Price-Weller-Pinkel) - This model consists of a mixed layer where the buoyancy is mixed completely each time step (Price, Weller and Pinkel, 1986). The thickness of the mixed layer is determined by a bulk Richardson number closure ($Rb \geq 0.65$), followed by a smoothing below the mixed layer to relieve any shear instabilities such that the local gradient Richardson number $Rg \geq 0.25$. This version, coded by Jim Price and modified by Glenn Flierl, also has an option for a background diffusion which was not used except by R. Hood who was using a version modified by Hood and Olson to correct problems with the coding of the background diffusion.
- MY (Mellor-Yamada) - This model is based on a level-2 turbulent closure scheme outlined in Mellor and Yamada (1974) and first implemented by Mellor and Durbin (1975). The vertical mixing at any depth is determined by a turbulent eddy coefficient that is a function of the mean turbulent kinetic energy (TKE), a length scale taken to

be the first moment of the TKE, and a stability coefficient that is calculated according to some laboratory-determined empirical equations that are functions of the local flux Richardson number Rf. Thus, an output of the model is a vertical profile of the coefficient of vertical turbulent diffusion of heat, $K_T(z)$, which is the key output for coupling with a biological model. This version, coded by Patrice Klein and modified by Jim Price, also has a constant background diffusion.

These three models were set up for the workshop by Glenn Flierl, with a common module for wind and heat forcing and a common biological NPZ module for coupling. A simple-to-use set of plotting commands was also set up so that comparison on common axes at the same size could easily by made.

- NCAR - This model was implemented and coupled to an NPZD at the meeting by S. Doney and D. Glover. This is a one-dimensional coupled biological–physical model built at NCAR as the first part of a longer term project for developing a 3-D, global coupled model. The physical model, which is based on models of the atmospheric planetary boundary layer, differs from existing ocean models, and a complete description can be found in Large et al. (1993). The model is a non-local parameterization of the oceanic boundary layer based on the concept that the profiles of eddy diffusivity in the planetary boundary layer (either atmosphere or ocean) are similar in shape if the appropriate scaling is applied (boundary layer depth, surface wind stress and surface buoyancy flux). The shape parameterization used in the model is based on Large Eddy Simulation (LES) results (Deardorff, 1972). Constraints are also applied to the parameterization such that the eddy diffusivity in the surface layer matches the results of similarity theory. The depth of the ocean boundary layer depth is computed based on a bulk Richardson number criteria.

  The physical model can be run using either prescribed surface fluxes or atmospheric state variables (e.g. air temperature and humidity, wind speed); atmospheric forcing can be either specified using simple harmonics or read in from a data file. The daily cycle of solar radiation is computed using a geometric solar model and the cloud model of Smith and Dobson (1984).

### 3.1.3 Biological models

The NPZ model set up on the computer by Flierl for coupling to the mixed layer models was a relatively simple model with some non-standard terms such as the extra P factor in the grazing term (to replace a threshold value in the Ivlev formulation), the Michaelis-Menten phytoplankton growth dependence on light, and the $Z^2$ dependence death term for the zooplankton. The model consisted of the following equations:

$$\frac{DP}{Dt} = V_m \frac{I_0(t)I(z)}{I_0(t)I(z) + \beta} \frac{N}{k_s + N} P - R_m \lambda P Z[1 - \exp(-\lambda P)] - bP$$

$$\frac{DZ}{Dt} = \gamma R_m \lambda P Z[1 - \exp(-\lambda P)] - dZ^2 \tag{1}$$

$$\frac{DN}{Dt} = -\frac{DP}{Dt} - \frac{DZ}{Dt}$$

where I(z) is the light intensity function

$$I(z) = \exp(z/\beta_2)$$

The surface light intensity $I_0(t)$ varied with time of day and season. Parameters values and initial conditions are given in Table I.

Table I. Parameter values used in the NPZ model set up by Glenn Flierl

| Parameter | Value | Description |
|---|---|---|
| $I$ | — | irradiance |
| $V_m$ | 2.0 | maximum phytoplankton growth rate |
| $k_s$ | 0.1 | nutrient half saturation coefficent |
| $R_m$ | 0.35 | maximum zooplankton growth rate |
| $\lambda$ | 1.0 | Ivlev coefficent |
| $b$ | 0.05 | phytoplankton mortality |
| $\gamma$ | 0.7 | egestion fraction |
| $d$ | 0.2 | zooplankton mortality |
| $\beta$ | 0.5-1.5 | light half-saturation coefficient |
| $\beta_2$ | 20. | light e-folding depth |

State Variables:   $P_0 = 2.7$   $Z_0 = 0.35$   $N_0 = 1.95$

Two other biological models were used as well. The NPZD model used by Hood consisted of a detrital compartment (D) added to the Flierl and Davis (1993) NPZ model (see section 3.1.7).

The biological model used by Doney/Glover was similar and was a nitrogen based flow model adapted from Fasham's model of the mixed layer (Fasham et al., 1993). The model is quite flexible in that the flow pathways and model parameters are specified as part of an input file at run time. Currently, the model is formulated as NPZD model and includes both turbulent transport and sinking of the biological components. Coupling between the biological model and the physical model via the absorption coefficient for solar radiation can also be included.

The general equation for any biological scalar at a particular grid level is:

$$\frac{dX}{dt} = -\frac{d\overline{w'X'}}{dz} - \frac{dw_{\text{sinking}}X}{dz} + \text{biology}$$

where $\overline{w'X'}$ is the turbulent flux of $X$ and $w_{\text{sinking}}$ is the sinking velocity of species $X$.

The biological production and consumption terms for the NPZD model are:

$$\frac{dP}{dt} = V_m(I)\frac{PN}{k_s + N} - R_m(1 - e^{-\lambda})Z - \epsilon P$$

$$\frac{dZ}{dt} = \gamma R_m(1 - e^{-\lambda})Z - gZ$$

$$\frac{dN}{dt} = -V_m(I)\frac{PN}{k_s + N} + mD \tag{2}$$

$$\frac{dD}{dt} = (1 - \gamma)R_m(1 - e^{-\lambda})Z + \epsilon P - mD + gZ$$

where parameter values are given in Table II.

Table II. Parameter values used in the Doney and Glover NPZD model.

| Parameter | Value | Description |
|-----------|-------|-------------|
| $I$ | — | irradiance |
| $V_m$ | 2.0 | maximum phytoplankton growth rate |
| $k_s$ | 0.1 | nutrient half saturation coefficent |
| $R_m$ | 1.0 | maximum zooplankton growth rate |
| $\lambda$ | 0.3 | Ivlev coefficent |
| $\epsilon$ | 0.1 | phytoplankton mortality |
| $\gamma$ | 0.7 | egestion fraction |
| $g$ | 0.2 | zooplankton mortality |
| $m$ | 1.0 | detrital remineralization rate |

### 3.1.4 *Tasks attempted and completed*

- The group explored and compared the behavior of the CONV, PWP and MY mixed layer models. They compared the shape of the vertical temperature profile, the annual cycles of surface temperature and mixed layer depth, conservation of heat and the vertical diffusion characteristics.
- The NPZD models were coupled first with CONV and parameters were adjusted to find 'stable' behavior, i.e. behavior that did not include inherently biological limit cycles, but rather annual cycles controlled by a combination of the annual cycles in solar radiation and mixed layer behavior.
- For the 'stable' parameter sets, the NPZ model was coupled to MY and the behavior compared with that of the coupled CONV - NPZ model.

8

- Similar runs were conducted with the NPZ model coupled to the PWP model
- The NCAR model was implemented with an NPZD model and tested with several multiyear simulations to demonstrate the influence of the detritus loop.
- An NPZD model was coupled to the CONV model and parameter space explored. A modified NPZD model was coupled with the Hood/Olson version of PWP.

### 3.1.5 Results of the comparison of mixed layer models

The PWP and CONV models behave very similarly, in terms of the annual cycle of sea surface temperature, mixed layer depth, and temperature profile.

Initially, the MY model did not conserve heat, but rather it added significant heat beyond the net heat input across the air-sea boundary, which was evident in both the annual SST cycle and the vertical profiles departing from those of CONV and PWP. (Figs. 1 and 2).

MY includes a bottom boundary layer and a background constant diffusion, initially set at $1.34 \times 10^{-5}$ m$^2$ s$^{-1}$. Over an annual cycle a large amount of heat was diffused from the mixed layer into the layer below, especially the bottom well-mixed layer. The extent of this diffusion is shown in a 2-year run where the surface heat exchanges were turned off (Fig. 3). The background diffusion dominated the modelled diffusion resulting from the level-2 closure as shown in Fig. 4, which is a plot of the $K_T(z)$ profile on a log$_{10}$ plot after 200, 360 and 850 modelled days (day 1 = 120).

The non-conservation of heat was traced to a function that was applied each timestep to keep the odd and even time leapfrog solutions from diverging from each other. G. Flierl replaced the scheme with a 1/2 timestep Euler solution every 100 timesteps, i.e. twice a day. The annual cycles of SST in CONV and MY then were almost identical (Fig. 5), where the background diffusion and the bottom boundary layer in MY were both turned off.
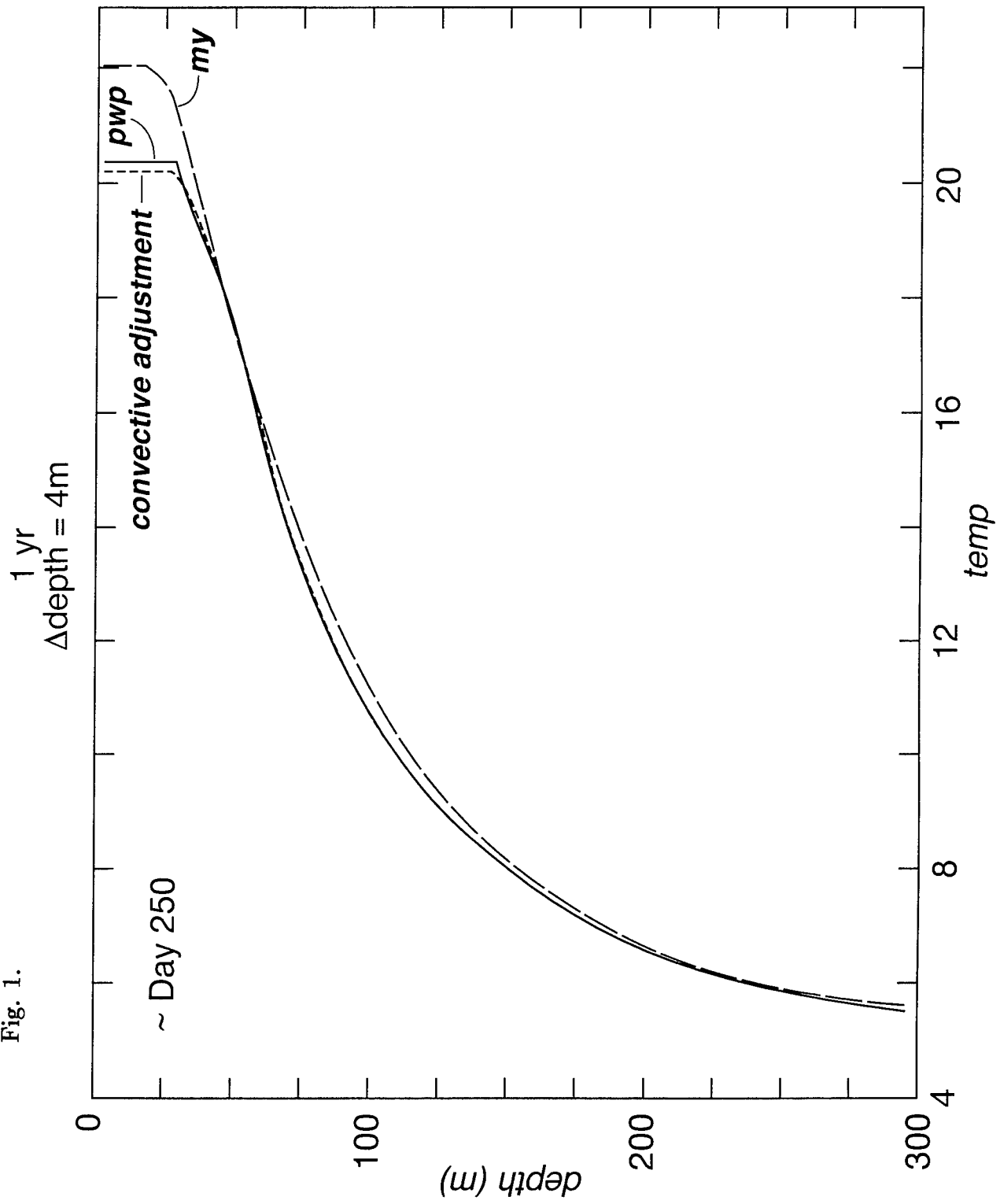
Another feature of MY is that convective mixing due to heat loss at the sea surface takes several timesteps to reach full adjustment for a deep mixed layer, unlike PWP (and CONV) where complete mixing occurs each time step. This behavior will generate propagating waves when PWP is embedded in a circulation model and adjacent gridpoints mix suddenly to different depths. However, the MY model appeared to take close to 10 times the computer time of PWP, so it may not be practical for inclusion in large high resolution 3D circulation models.

The NCAR mixed layer model, based on a fitted similarity solution for the vertical profiles of $K_T$, is an attractive option. Its ability to simulate a stable annual cycle in the mixed layer is shown in Fig. 6.

As part of the workshop, the NCAR model was transferred to and adapted to run on the NASA EOS interdisciplinary team SCF SGI at WHOI. Using a set of simple, harmonic forcing functions, we generated a physical model solution for a Sargasso Sea like case (Fig. 6a and b). The model produced deep, convective mixing during winter and a shallow mixed layer and seasonal thermocline of approximately the correct amplitude during the summer. A distinct and stable seasonal cycle developed after one year. Notably, the model retains a thick layer of mode water at about eighteen degrees.

### 3.1.6 Results with coupled NPZD and mixed layer models

Fig. 1.

1 yr
Δdepth = 4m

~ Day 250

convective adjustment

pwp

my

temp

depth (m)

10

Fig. 2.

11

Fig. 3.

µmol = 1.34 x 10⁻⁵

no heating

day 120

day 850

temp

depth (m)

12
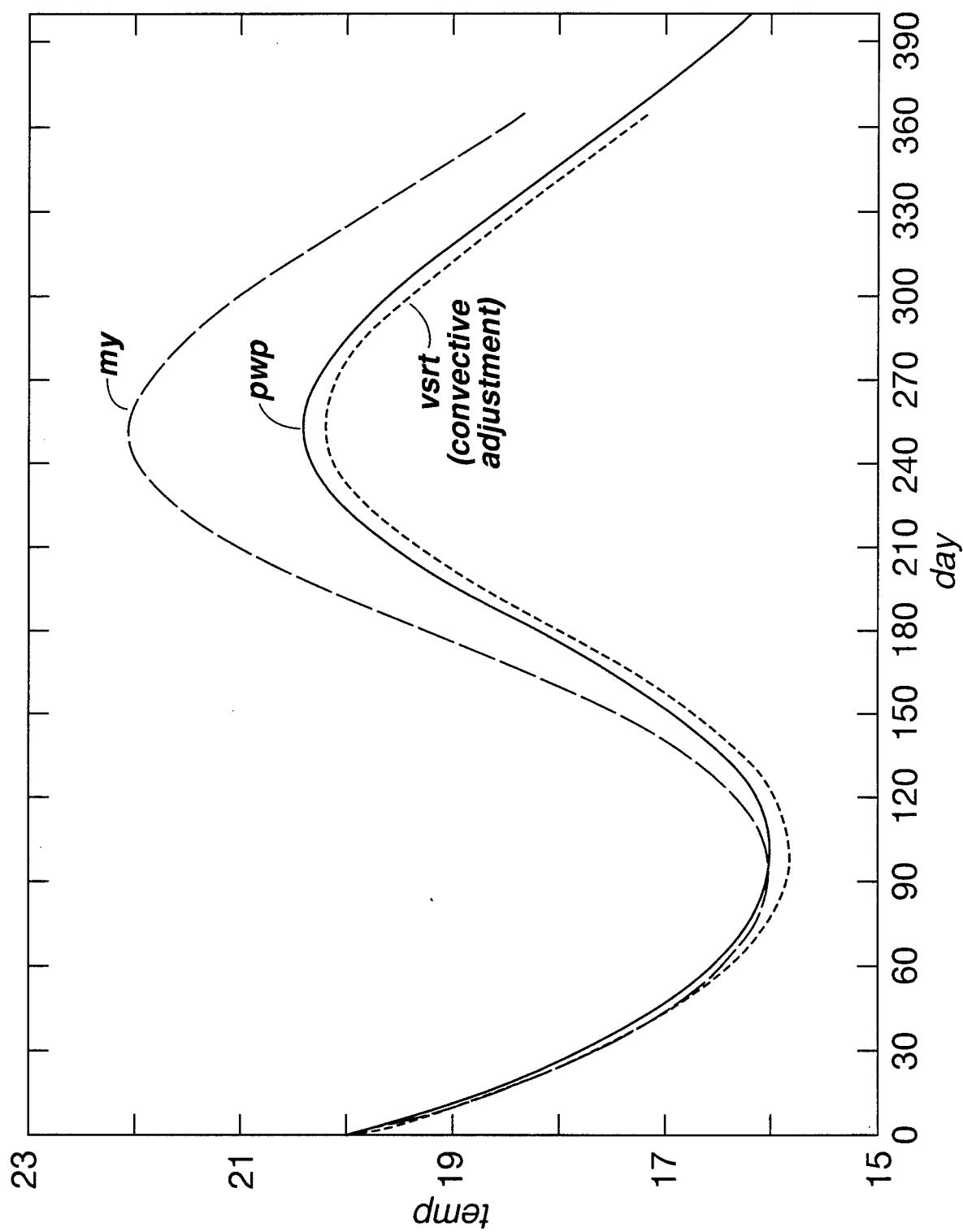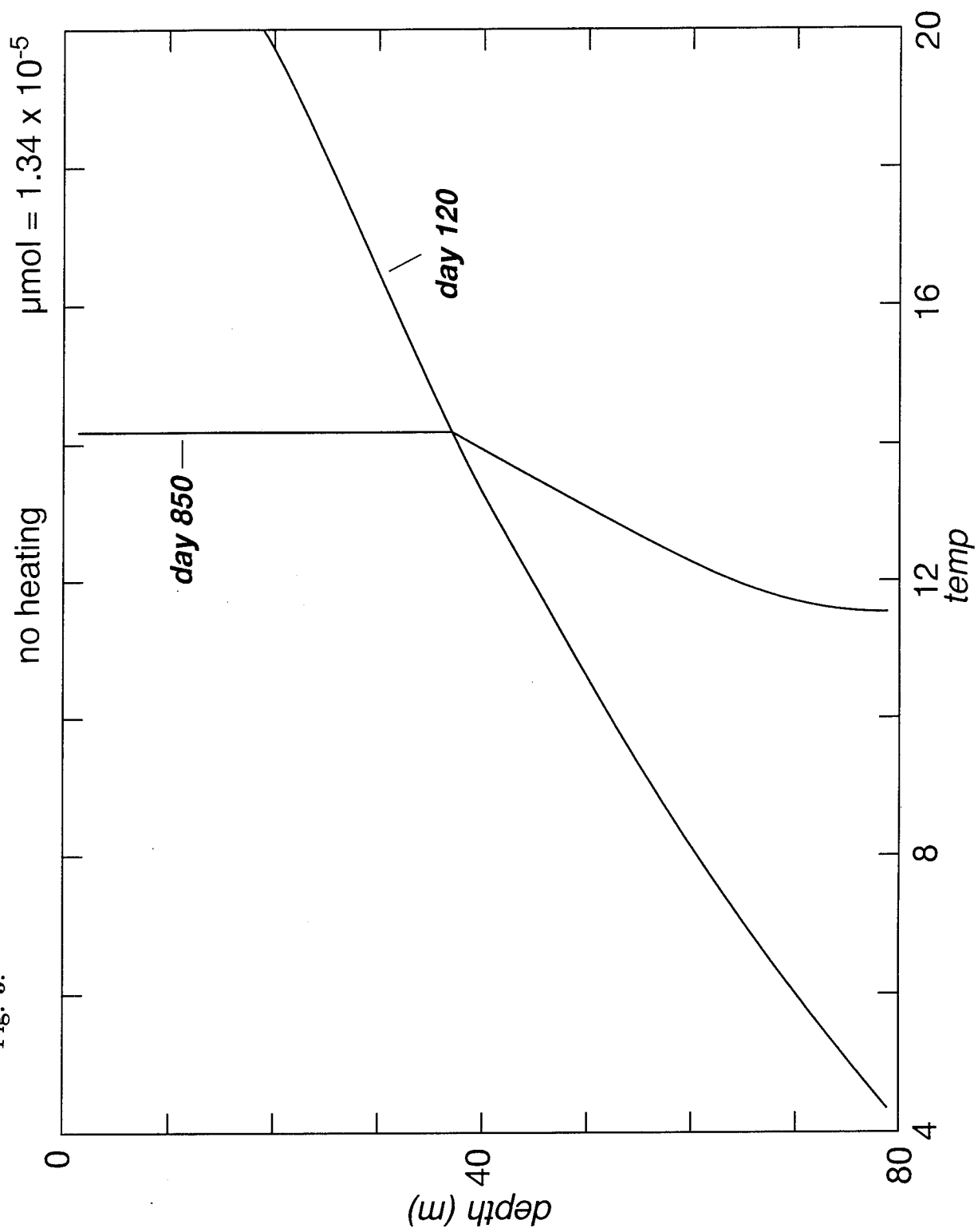
day 1 = 120
depth > 5 m

Fig. 4.

13

Fig. 5.

depth = 1 m

convection
my

14

Fig. 6. NCAR K-profile model run for three years at a Sargasso Sea like location (64°W, 32°N) showing model stability for both (a) temperature (°C) and (b) phytoplankton (mM N m$^{-3}$).

Fig. 6b.

# Phytoplankton (2m/d sinking)

16

The NPZ model coded by G. Flierl was coupled first to the CONV model and parameter space was explored. Initially, interesting behavior resulted where several Lotka-Volterra like limit cycles occurred each spring-summer-autumn period, exhausting nutrients briefly each cycle. These were slowed down, by changing the parameters, to 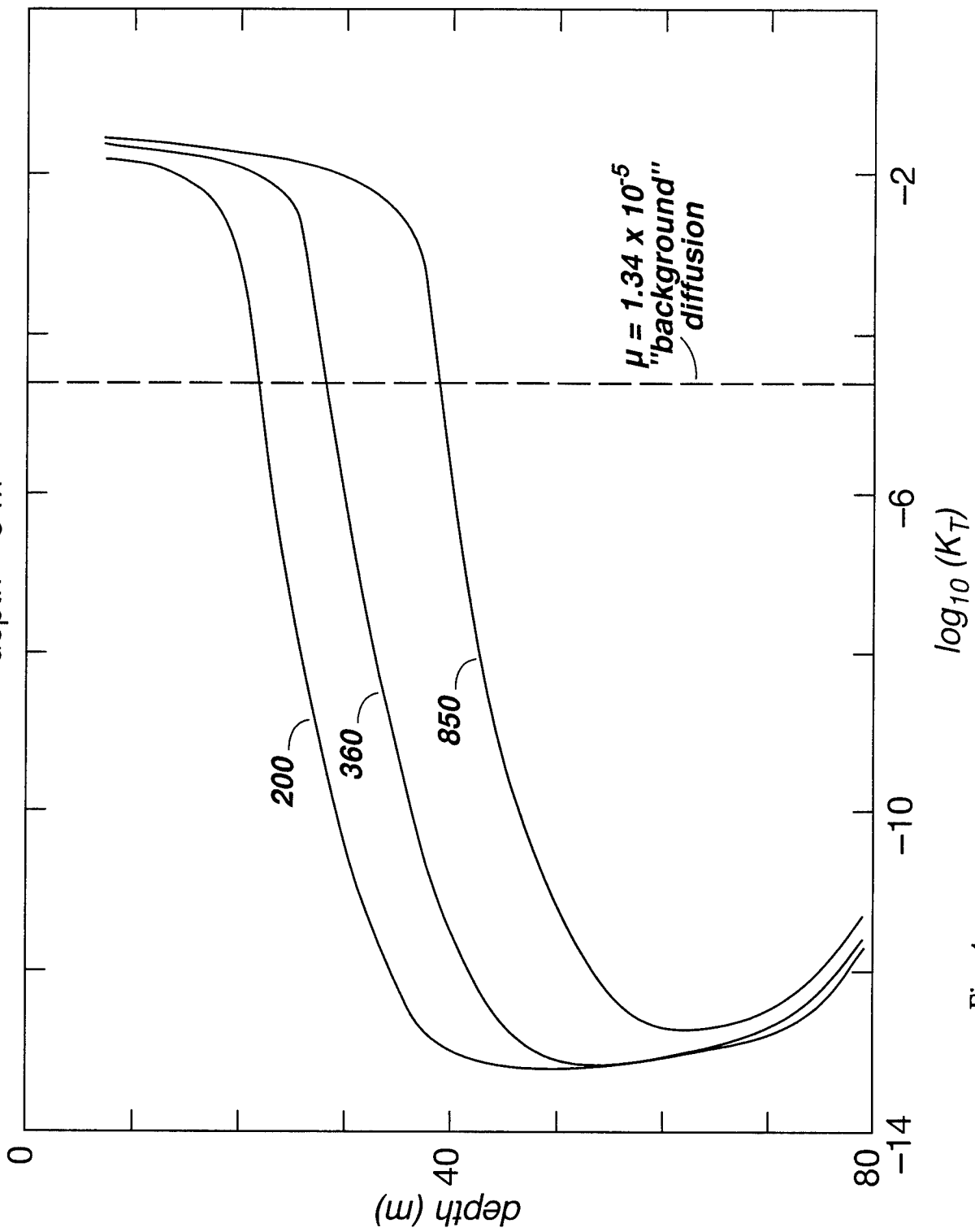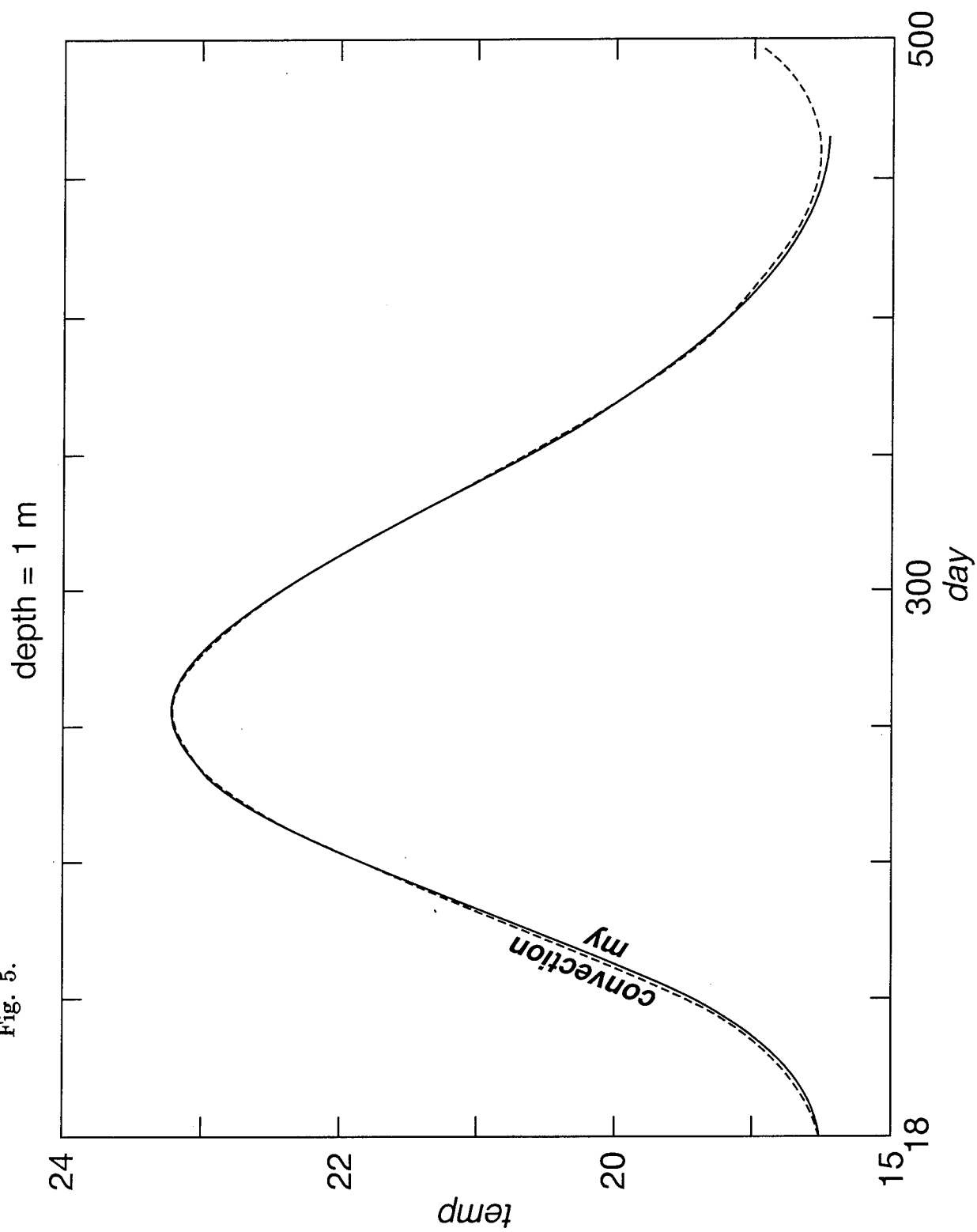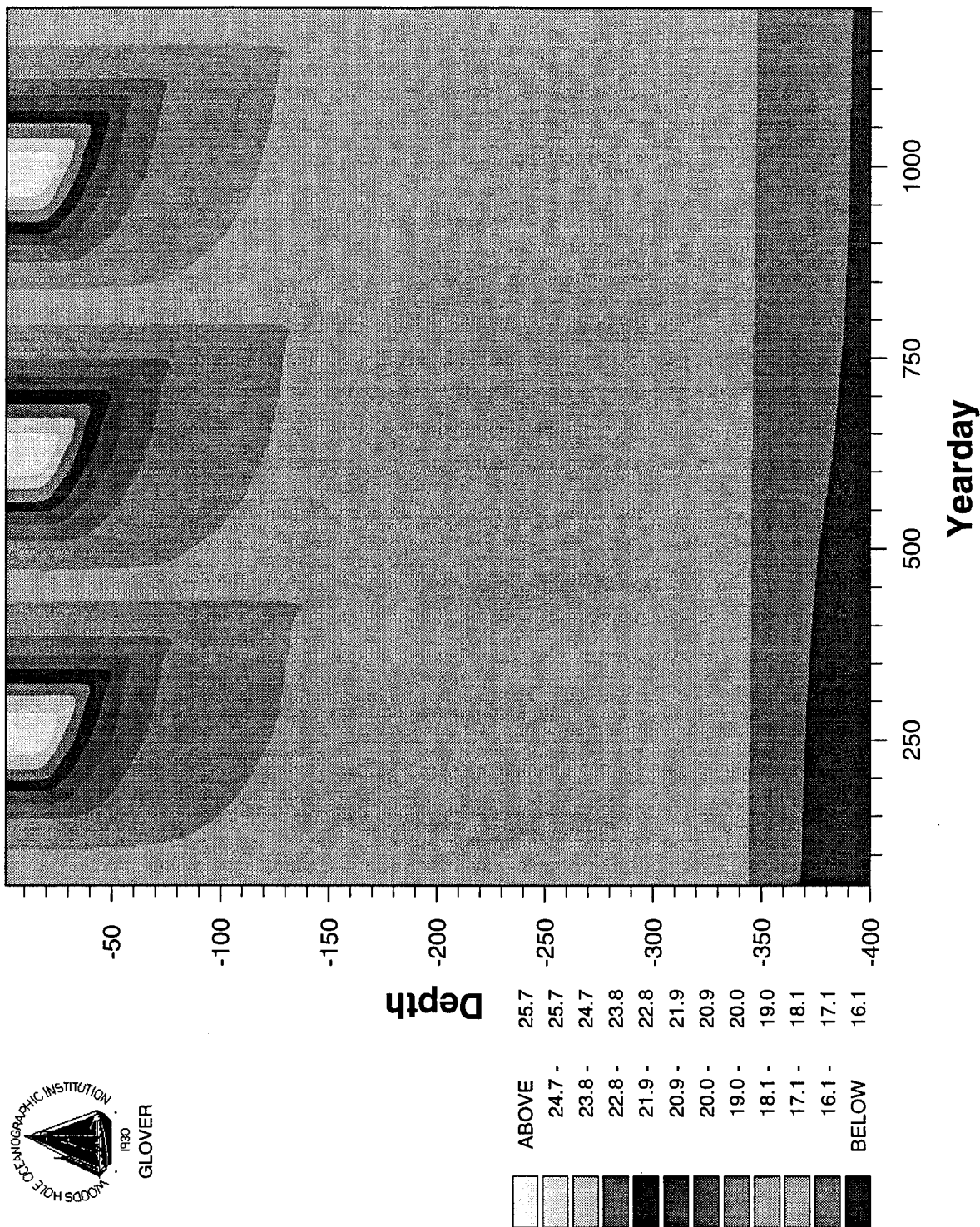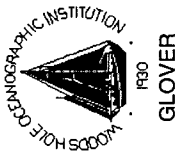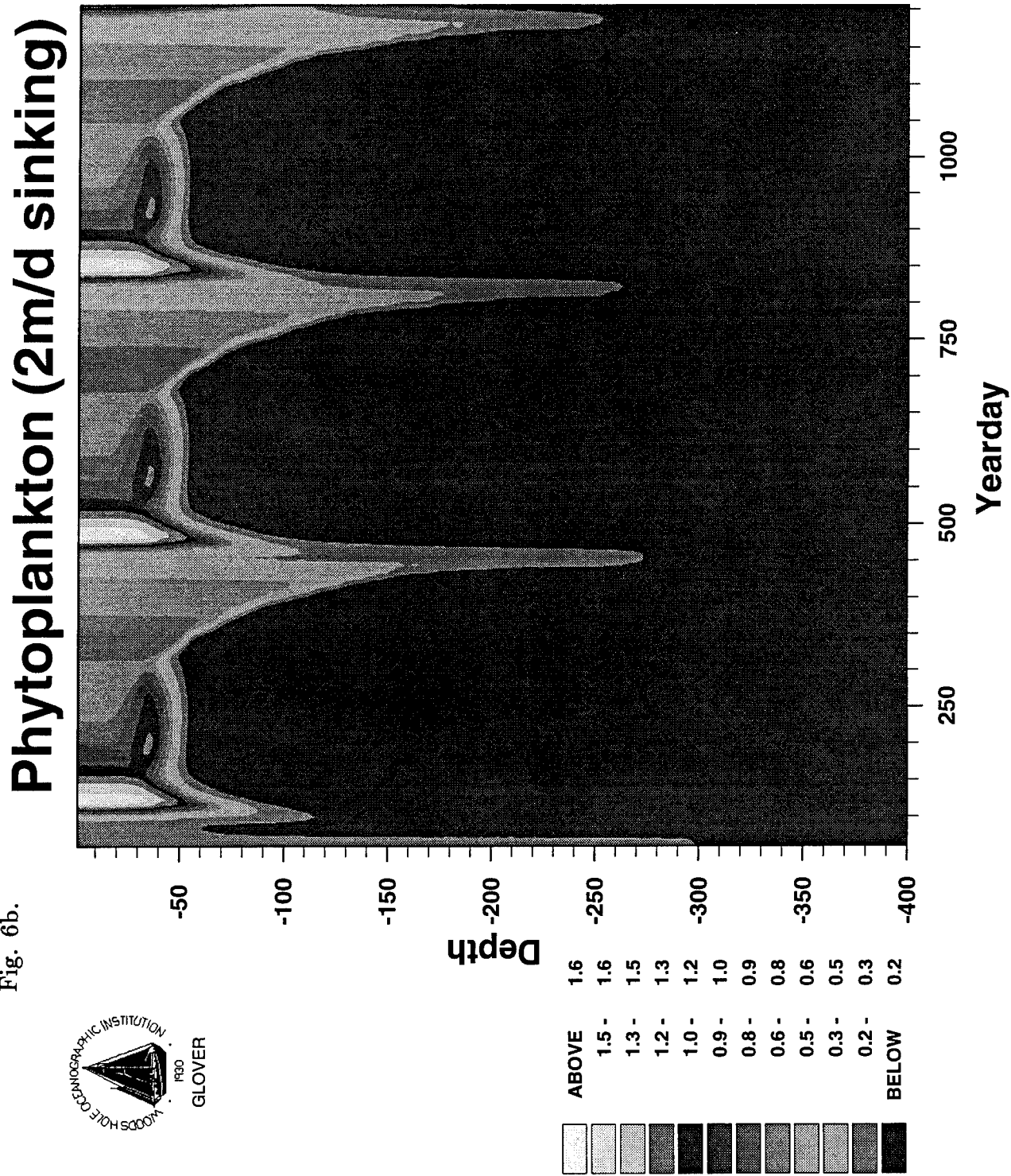about one per year. The spring phytoplankton bloom progressed downward with time until it got below the mixed layer where for some parameter sets, limit cycles occurred as the peak in P and Z slowly propagated to the bottom.

Finally, two sets of parameters were found which produced well-defined annual cycles. One without a spring bloom ($\beta = 0.5$) was characteristic of the annual cycle in the subarctic North Pacific Ocean in the vicinity of the former ocean station P. (see Fig. 7). The other set of parameters, with a lower initial slope of the P-I light response curve ($\beta = 1.5$), produced a short spring bloom, apparently because of a much smaller overwintering zooplankton population, less able to crop the increase in phytoplankton growth as the mixed layer shoals. (see Fig. 8). (In both figures the initial oscillations result from the initial conditions.)

The NPZ model coupled with the MY mixed layer model (Figs. 9, 10) reveals that the biological variables behave almost exactly like in the CONV models, given that the annual cycle of the mixed layers in the two models is different. In MY the mixed layer reached the bottom of the model at 80 m each winter and the summer mixed layer was not as shallow.

The original form of CONV indeed had a 30m mixed layer depth. For the particular forcing function, however, the PWP and MY models seemed to have a summer MLD of about 10m, so the parameters for CONV were changed to use this value.
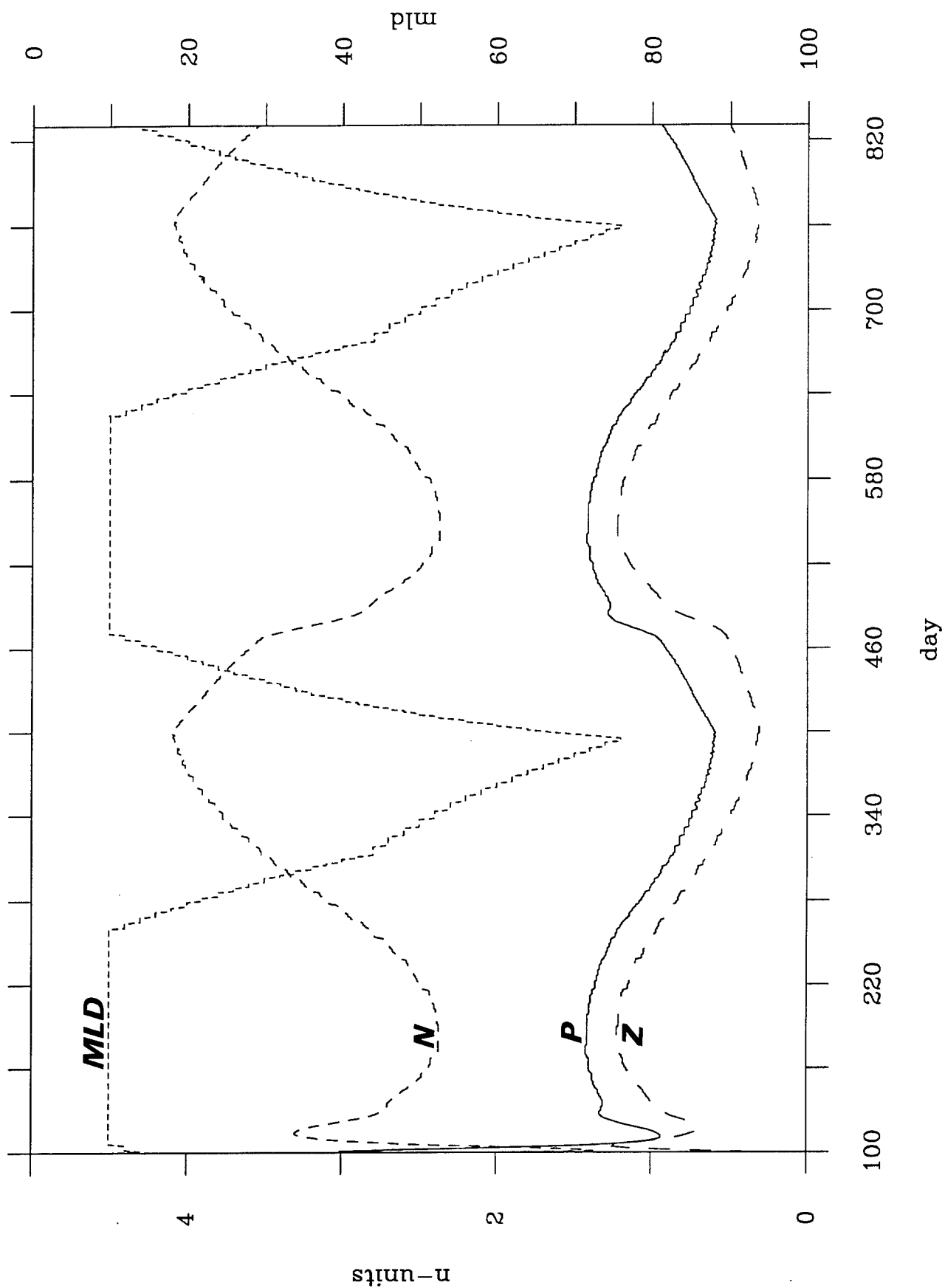
An NPZ model from Peter Franks, adapted to include detrital material (see below), was used during the workshop to test the sensitivity of simple models to detrital sinking. The remineralization of the detrital particles is treated as a simple first order process. The NPZD models solutions, shown in Figs. 11 and 12, were run both with and without detrital sinking (2 m/day), and the total nitrogen content of the surface layer is 2 mmol m$^{-3}$, similar to that for Bermuda. Both models predict a strong spring bloom in both phytoplankton and zooplankton with very low nutrients during the summer. Adding detrital sinking modifies the model solution in several fashions: surface zooplankton and phytoplankton concentrations are lower in the summer, a fall bloom occurs in the sinking case when fall mixing entrains nutrients into the mixed layer, and a subsurface nutrient maximum develops in the seasonal thermocline due to detrital remineralization. The subsurface nutrient maximum appears to be an unrealistic feature of the model, resulting from too shallow of a remineralization scale.

### 3.1.7 A coupled PWP + NPZD model

Hood, Olson, Flierl

A detritus compartment ($D$) was added to the Flierl and Davis (1993) $NPZ$ biological model (see Table III) and then forced with a modified version of the Price, Weller and Pinkel (1986) mixed layer model (see description of the Hood/Olson PWP-NPZD model in Appendix III.C. for details). The additional detritus compartment can be considered a

17

Fig. 7.

Conv (No bloom)



18

Conv (Bloom)

Fig. 8.

19

M–Y (no bloom)

Fig. 9.

MLD

N

P

Z

day

mld

n–units
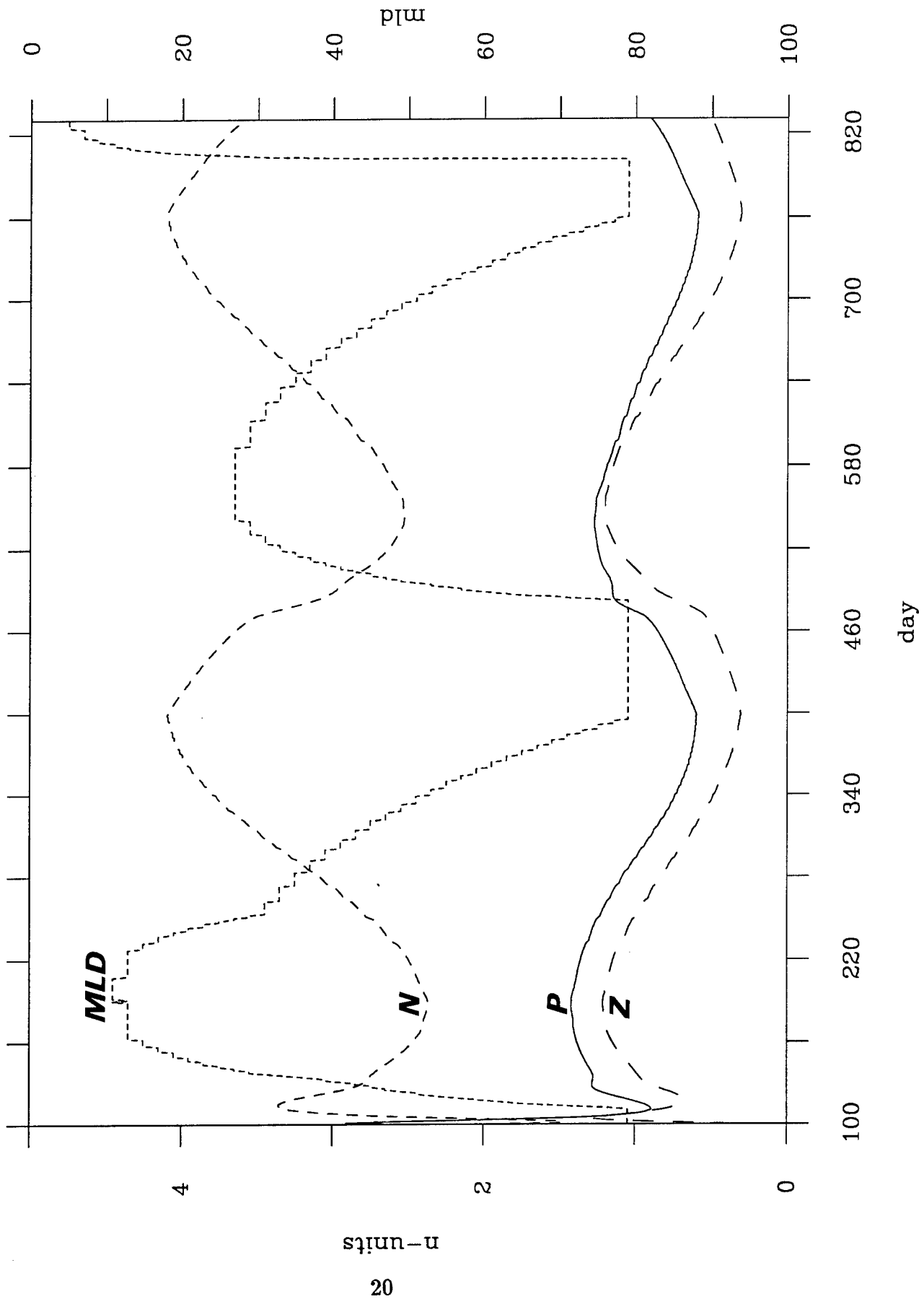
20

M-Y (bloom)



Fig. 10.

21
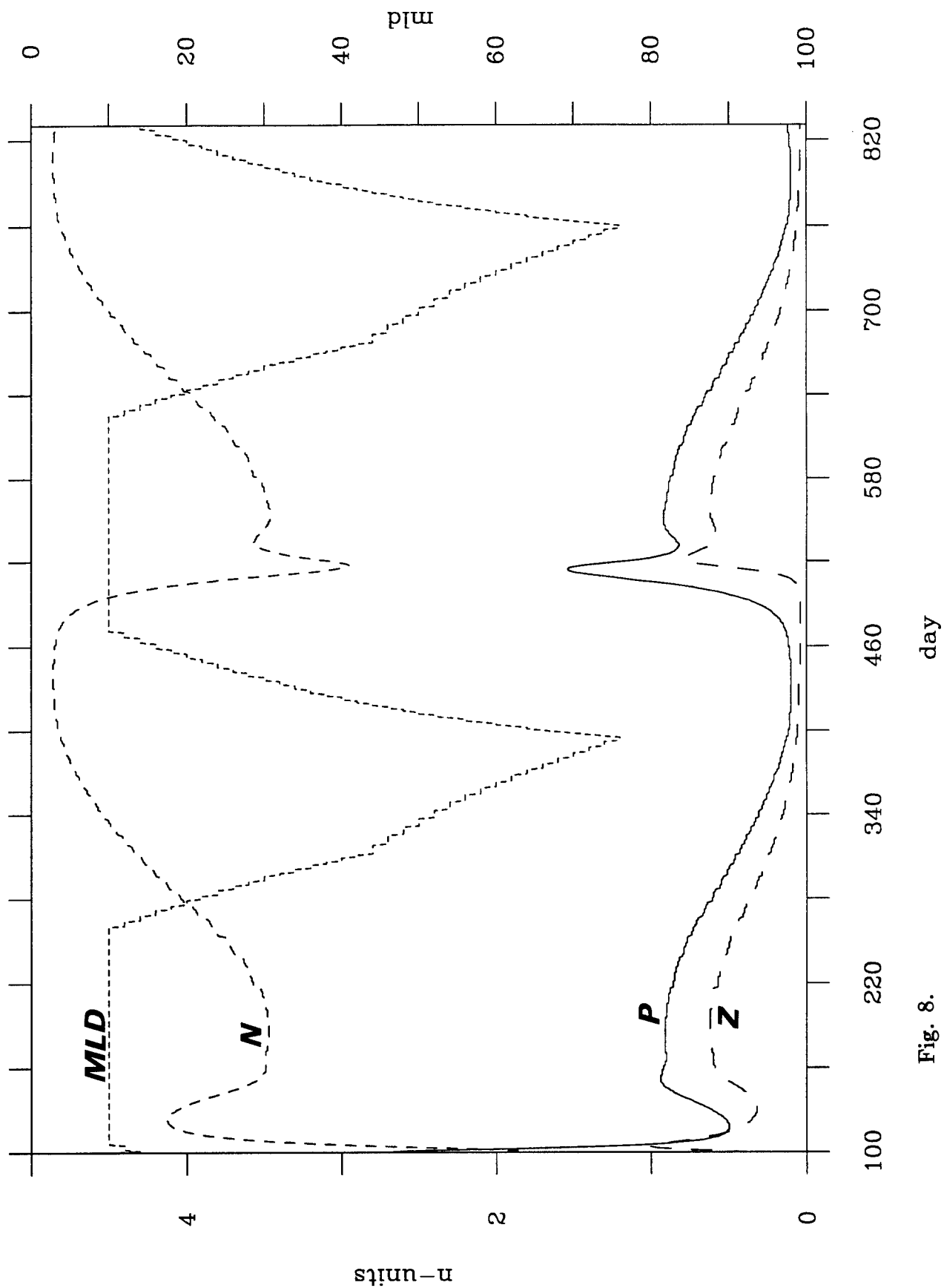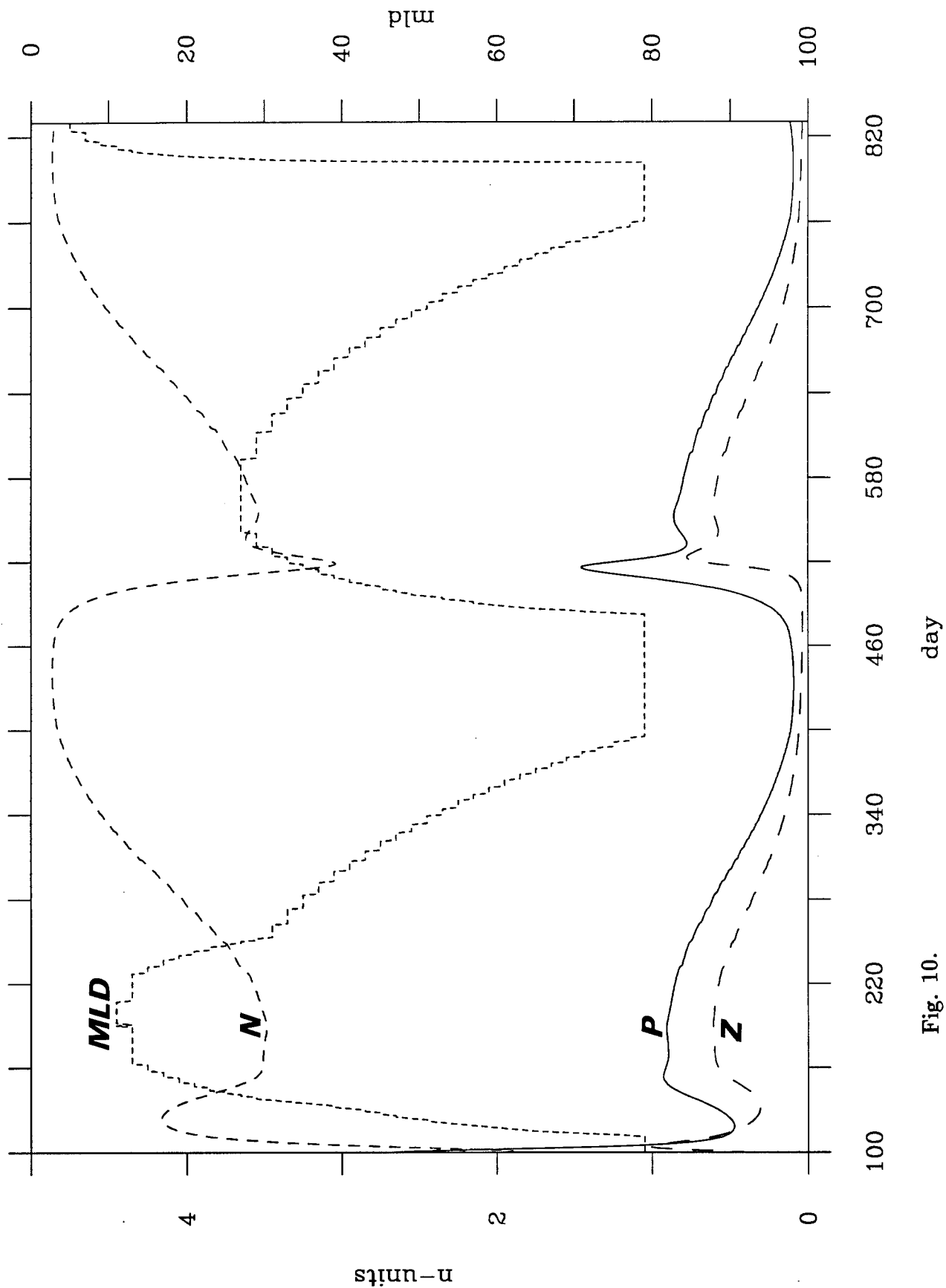
# Phytoplankton (no sinking)
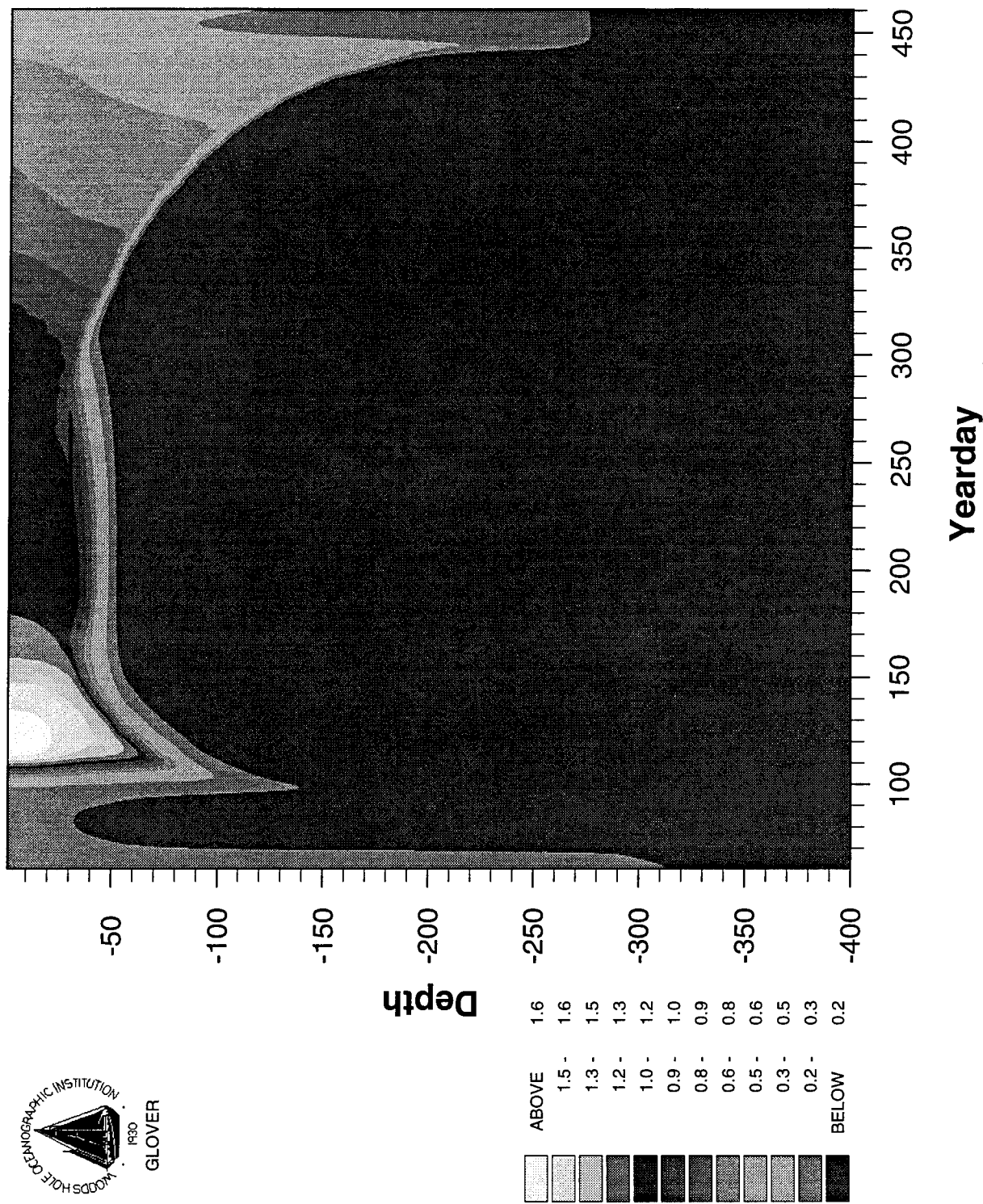


Fig. 11. NPZD/K-profile model solution for phytoplankton (mM N m$^{-3}$) for a Sargasso Sea location (64°W, 32°N) with no sinking.

22

# Phytoplankton (2m/d sinking)
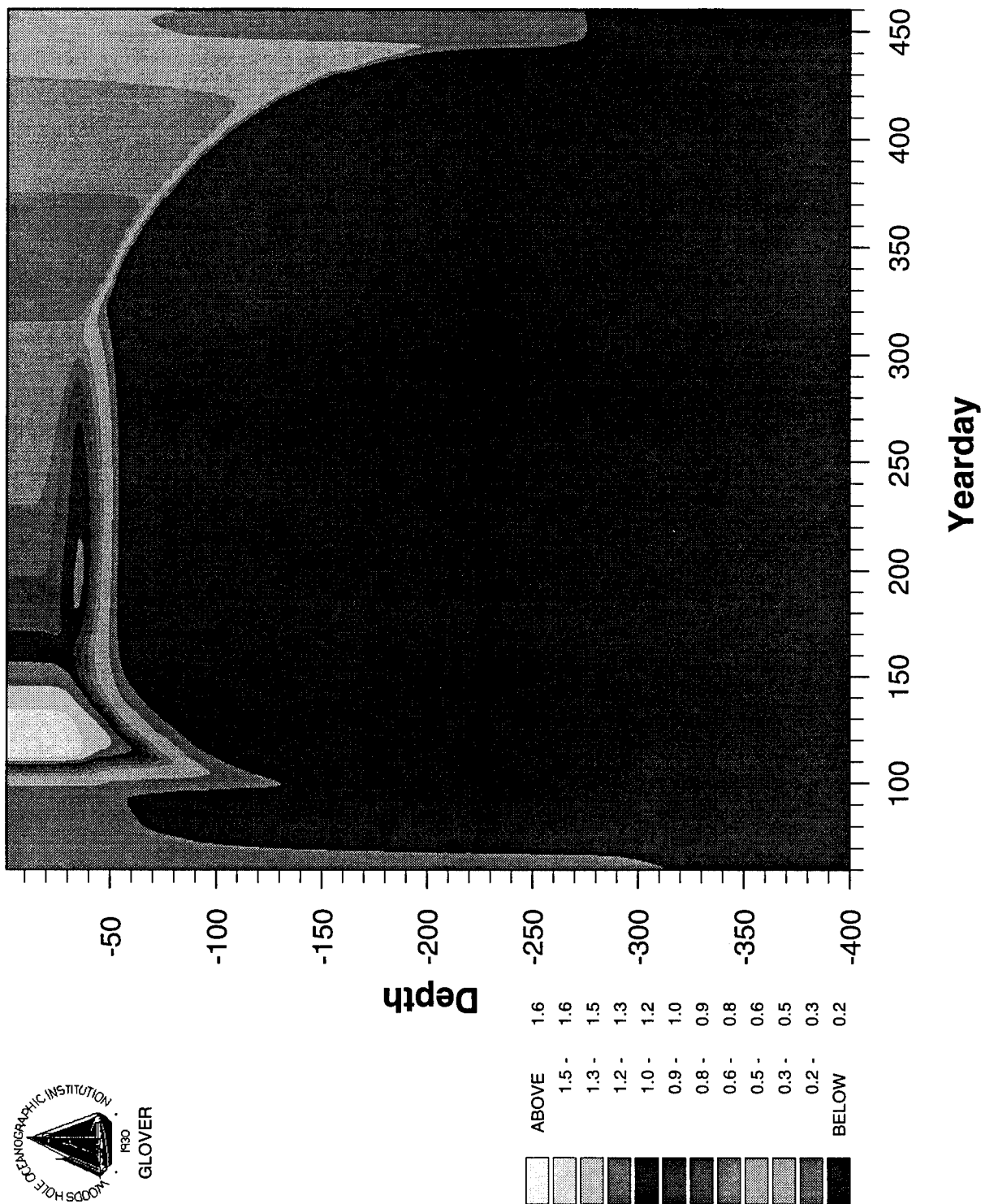


Fig. 12. NPZD/K-profile model solution for phytoplankton (mM N m$^{-3}$) for a Sargasso Sea location (64°W, 32°N) with sinking (2 m d$^{-1}$).

Table III. Hood/Olson NPZD equations, variables, and parameters.

**The model:**

$\dot{P} = uptake - grazing - pd \times P$

$\dot{Z} = ga \times grazing - zd \times Z$

$\dot{N} = (ae - ga) \times grazing - uptake + Ae \times zd \times Z + e \times D$

$\dot{D} = (1 - ae) \times grazing + (1 - Ae) \times zd \times Z + pd \times P - e \times D$

$grazing = Rm \times P \times Z \times \lambda \times (1 - e^{-\lambda P})$

$uptake = Vm \times P \times \left(\frac{N}{N + Ks}\right) \times \left(\frac{I}{I + \beta}\right)$

**Variables and Coefficients:**

| Description | Symbol | Value/Units |
|---|---|---|
| Dissolved nitrogen | $N$ | $\mu$M |
| Phytoplankton nitrogen | $P$ | $\mu$M |
| Zooplankton nitrogen | $Z$ | $\mu$M |
| Detritus nitrogen | $D$ | $\mu$M |
| Light intensity | $I$ | dimensionless |
| Max. phytoplankton growth rate | $Vm$ | $0.3/day$ |
| Max. zooplankton Grazing rate | $Rm$ | $0.7/day$ |
| Zooplankton Death rate | $zd$ | $0.05/day$ |
| Detritus remineralization rate | $e$ | $0.2/day$ |
| Phytoplankton scenscence rate | $pd$ | $0.05/day$ |
| Growth efficiency for Z | $ga$ | 0.35 |
| Assimilation efficiency for Z | $ae$ | 0.70 |
| Assimilation efficiency for higher trophic levels† | $Ae$ | 0.70 |
| Half saturation constant for N | $Ks$ | $0.1\mu$M |
| Half saturation constant for I | $\beta$ | 0.01 |
| Saturation constant for grazing | $\lambda$ | $3.5/P$ |

† Growth efficiency for higher trophic levels set at zero

simple "microbial loop", where the detrital remineralization rate ($e$) is the rate at which bacteria convert detrital Nitrogen to dissolved Nitrogen.

Before running the coupled model we (Steele, Davis, Flierl, Olson and Hood) chose a set of coefficients for the biological model (Table III). Most of these are accepted values for diatom/copepod dominated food webs, based upon observational and experimental data. No clear consensus was reached as to the proper magnitudes of the zooplankton death rate ($zd$), the detritus remineralization rate ($e$), and the phytoplankton senescence rate ($pd$).

We forced the $PWP$ model with idealized functions for the Atlantic ocean at 20° N (Bleck et al., 1989), which resulted in seasonal variations in mixed layer depth between 10 and 100m. Under these forcing conditions the ecosystem model would not run with the coefficients set as above, primarily because the phytoplankton could not survive the winter-time deep mixing period. In order to overcome this problem it was necessary to increase the maximum phytoplankton growth rate ($V_{max}$), and to lower the half saturation constant for light, ($\beta$).

The coupled model is sensitive to the grazing formulation. With simple Ivlev grazing we were unable to find a set of model coefficients that gave a stable ecosystem over the entire range of physical variability. We therefore used a modified version of the Ivlev equation (see equations) that includes an additional linear dependence on $P$. With this grazing formulation temporal changes in phytoplankton and zooplankton biomass are much more tightly coupled. This damps oscillations and helps prevent runaway growth of phytoplankton in the summer and extinction in the winter. There are other, possibly better ways to prevent runaway growth and extinction. Some participants in the workshop recommended using the Ivlev formulation with a minimum grazing threshold (Moisan). Steele recommended using a formulation of the form $grazing = Rm(P^2/(1 + P^2))$, which results in reduced grazing pressure at very low phytoplankton populations. The incorporation of an additional phytoplankton species with different growth characteristics might be the most ecologically realistic way to solve the problem (e.g. include one species adapted to summer-time conditions and another adapted winter-time conditions).

Previous work by Hood and Olson has revealed that the diffusion subroutine in $PWP$ is nonconservative. We therefore recommend incorporation of a better numerical scheme (e.g. Crank-Nicholson).

### 3.2 *Food Webs*

Armstrong (Chair), Bollens, Frost, Landry, Landsteiner, Moisan

### 3.2.1 *Motivation*

Our overall objective was to construct a general model of a pelagic food web and to embed this model in an appropriate 1-dimensional physical model. Since several members of the group have extensive experience modelling the subarctic Pacific (e.g., Frost 1987; Miller et al. 1991), we decided to develop this model with explicit reference to OWS P. Two characteristic biogeochemical features of this region are that nitrate remains high ($>$5-7 mmol m$^{-3}$) and chlorophyll remains low ($<$1 mg chl $a$ m$^{-3}$) throughout the year (Miller et al. 1991). In addition, the phytoplankton are dominated by small ($<$20 $\mu$m) cells (Booth 1988), but blooms of large cells can be caused by addition of iron to natural

cultures (Martin et al. 1991). We wished to see under what circumstances a general pelagic food web model would reproduce these features.

### 3.2.2 *Model formulation*

The biological model was based on that of Frost (1987); that model was modified to include multiple size classes of both predators (zooplankton) and prey (phytoplankton and smaller zooplankton). The model could potentially support four size classes each of phytoplankton and zooplankton.

We considered four types of food webs (Fig. 13). The particular scenario we tested was whether, given realistic physical forcings for Station P, a multichain food web model would collapse to one containing only small phytoplankton species while allowing nitrate to remain high, or whether all four chains would persist, producing lower nitrate values than are typically observed. If the latter happened, we would then test whether adding a parameterized form of iron limitation (Armstrong, in press) would make the model behave more like the subarctic Pacific.

Nominal size classes for phytoplankton were set as 1, 4, 16, and 64 $\mu$m equivalent spherical diameter; zooplankton size classes were offset from those of phytoplankton by one length unit at 4, 16, 64, and 256 $\mu$m. Rate constants for phytoplankton and zooplankton in different size classes were assumed to follow allometric (power law) relationships so that the rate constant $R_i$ for the $i$th size class is related to that of the next smaller size class by

$$R_i = R_{i-1} \left( L_i / L_{i-1} \right)^{\beta_R} \tag{1}$$

where $L_i$ is the characteristic size (length) of size class $i$ and $\beta_R$ is the allometric constant associated with rate process $R$ (Moloney and Field 1989, 1991). Mesozooplankton (predominantly copepods in the genus *Neocalanus* were included as upper level predators, consuming all other elements of the food web except the smallest algal size class. Nitrogenous substrate ("nitrate") was assumed to be conserved in the system, with instant remineralization to nitrate upon death of one of the living components. Bacteria were excluded from consideration since their inclusion would have required differentiating ammonium from nitrate so that the balance of nutrient regeneration (as ammonium), export (as one or more forms of organic nitrogen), and import (as nitrate from depth) could be explicitly modelled. The defining equations for the growth of phytoplankton ($P_i$) and zooplankton ($Z_j$) are

$$\frac{dP_i}{dt} = \mu_i P_i - \sum_{Z_j \text{ eating } P_i} Z_j \frac{P_i}{F_j} H_j \left( F_j \right) - \lambda_i P_i \tag{2}$$

and

$$\frac{dZ_j}{dt} = Z_j \gamma_j H_j \left( F_j \right) - \sum_{Z_k \text{ eating } Z_j} Z_k \frac{Z_j}{F_k} H_k \left( F_k \right) - \lambda_j Z_j \tag{3}$$

In these equations $F_j$ is the food available to zooplankton size class $j$; it is calculated as the unweighted sum of the densities (measured as nitrogen equivalents) of all size classes
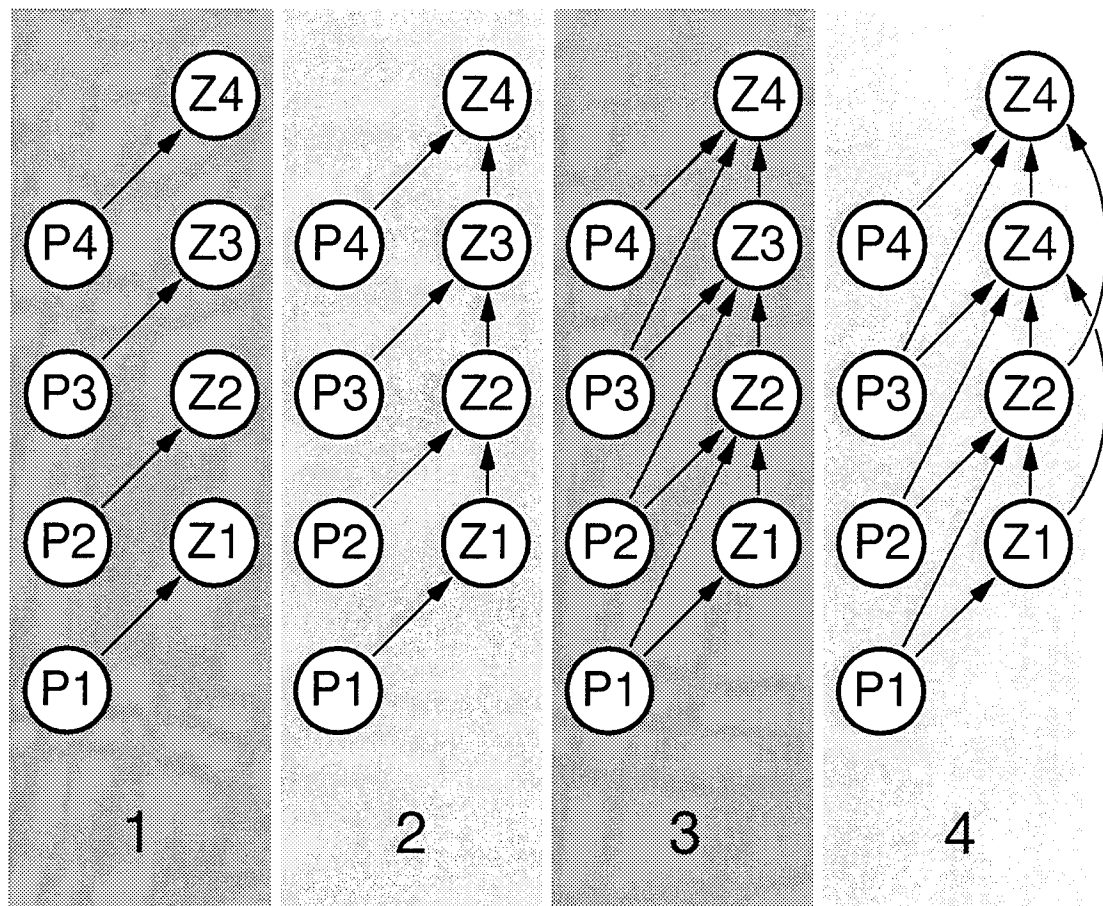
26

Fig. 13.

of phytoplankton and zooplankton preyed upon by zooplankton size class $j$; this set differs among food webs (see Fig. 13). The total harvest rate $H_j$ of food by zooplankton size class $j$ was taken to be

$$H_j \;=\; H_{max,j} \; \frac{F_j \;-\; F_{thresh,j}}{K_{Z,j} \;+\; F_j \;-\; F_{thresh,j}} \;\;, \tag{4}$$

where $H_{max,j}$ is the maximum harvest rate [mmol prey (mmol $Z$)$^{-1}$ $d^{-1}$], $K_{Z,j}$ is the half-saturation constant for zooplankton feeding, and $F_{thresh,j}$ is a threshold food level at which feeding stops. In these equations, phytoplankton growth rate for size class $i$ ($\mu_i$) is also given as

$$\mu_i \;=\; \mu_{max,i} \; f_i(I) \; \frac{N}{K_{N,i} \;+\; N}, \tag{5}$$

where $N$ is nitrate concentration (mmol m$^{-3}$), $\mu_{max,i}$ is maximum growth rate (d$^{-1}$), $f(I)$ is the fraction of maximum growth allowed at light level $I$ (see pp. 52-54 of Frost 1987 for details), and $K_{N,i}$ is the half-saturation constant for nitrate uptake. Seasonal data on mesozooplankton abundance were combined with data on *Neocalanus* feeding rates (Frost 1987) to supply loss rates $\lambda_i$ and $\lambda_j$ according to Equations 23 and 24 of Frost (1987).

Total nitrogen ($N + \Sigma P_i + \Sigma Z_j$) was taken to be 11.5 mmol m$^3$. Simulation results were generated using physical forcings appropriate for Station P (Fig. 2 of Frost 1987). Values for critical parameters are listed in Table IV; all concentration units are nitrogen equivalents.

Table IV. Model parameters used in the food web simulations.

| Parameter | Value for smallest size class | Allometric coefficient |
|---|---|---|
| $\mu_{max,i}$ | 1.4 d$^{-1}$ @ 12°C | 0, -1 |
| $H_{max,j}$ | 2.0 d$^{-1}$ @ 5°C | -0.25 |
| $K_{N,i}$ | 0.2 mmol $m^3$0.1 | 0.5 |
| $K_{Z,j}$ | 0.13 mmol m$^3$ (10 $\mu$g Chl $a$ l$^{-1}$) | 0.5 |
| $F_{thresh,j}$ | 0.075 mmol m$^3$ (5 $\mu$g C l$^{-1}$) | 0 |
| $\gamma_j$ | 0.4 | 0 |

### 3.2.3 Results

Model runs were made with four different trophic structures (Fig. 13). Initial conditions were equal biomass concentrations in each size class of phytoplankton and each size of consumer. Each version of the model was run for several years until a steady annual cycle was obtained. The results illustrated below are steady annual cycles.

Model runs with trophic structures 1-3 predicted blooms of large-sized phytoplankton. Larger sizes of phytoplankton bloomed because the disparity between specific growth rates

28

of phytoplankton and those of their chief consumers increased with size. The timing of phytoplankton blooms depended on trophic structure. With trophic structure 1 a relatively small, brief bloom of large cells (P4) occurred at the time of spring restratification (Fig. 14); after the bloom phytoplankton stock remained low and nutrient concentration was high. The model with trophic structure 2 produced a succession of blooms - first a brief bloom of P2, then a brief bloom of P1, and finally a bloom of P3 that persisted throughout the summer and early fall (Fig. 15). In this case N was depleted in summer. Trophic structure 3 produced an annual cycle similar to that for trophic structure 1, namely, a small bloom at the time of spring restratification followed by a low chlorophyll-high N condition for the rest of the year (Fig. 16).

In runs of the model with trophic structures 1-3 the magnitude of phytoplankton blooms was increased by any process that reduced the growth rates of consumers relative to those of their prey organisms (e.g., an additional mortality rate imposed on all consumers, either as by a constant daily mortality, or predation by mesozooplankton). The magnitude of phytoplankton blooms was reduced somewhat by decreasing the allometric constant for half-saturation of ingestion by consumers (e.g., $\beta$ for $K_{Z,i}$ decreased to 0.25) or by introducing weak size-dependence of phytoplankton maximum specific growth rate (e.g., $\beta$ = -0.25 for $\mu_{max,i}$). However, blooms of large phytoplankton cells could be fully suppressed only under strong size- dependence of phytoplankton maximum specific growth rate, as might pertain under iron limitation. For example, with $\beta$ = -1.0 for $\mu_{max,i}$ the versions of the model with trophic structures 1-3 produced the year-round condition of low chlorophyll-high N observed in the open subarctic Pacific. The result for trophic structure 1 is shown in Fig. 17. In these runs of the model, one or two of the larger size classes of phytoplankton (P3, P4) were greatly reduced in abundance if not entirely lost.

The model results suggest that strong size-dependent limitation of phytoplankton specific growth rate is required to reproduce the low chlorophyll-high N condition observed in the open subarctic Pacific. However, the model with trophic structure 4 reproduced the condition without imposed limitation on growth rate of the large size classes of phytoplankton (Fig. 18). In the steady annual cycle the trophic structure reduced to a simple linear food chain consisting of P1 and two size classes of consumers (Z2 and Z4). Very similar results were also obtained when reasonable levels of mortality (either a constant daily mortality or predation by mesozooplankton) were imposed on all consumers. However, even with trophic structure 4 blooms of very large phytoplankters might be predicted if the model was extended to include one or two larger size classes of phytoplankton and consumers. Although this trophic structure seems most realistic (i.e., a consumer can ingest any trophic type of prey - phytoplankton or zooplankton - in the size classes utilizable by it), an elaboration of this trophic structure might be to assign to consumers variable ingestion efficiencies on different sizes of prey.

Predictions of the model with trophic structures 1-3 were not sensitive to the level of phytoplankton production. For example, increasing $\alpha$ (the initial slope of the photosynthesis vs. irradiance response of the phytoplankton) from 0.75 to 5.0 approximately doubled the annual phytoplankton production, but the seasonal cycles of abundance of phytoplankton and consumers were essentially the same as described above. In contrast, the same increase in a in the model with trophic structure 4 led to a large summer bloom
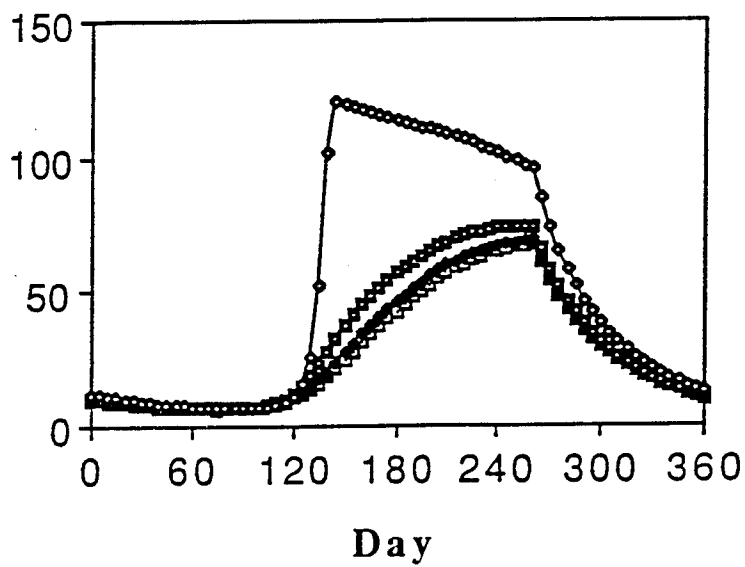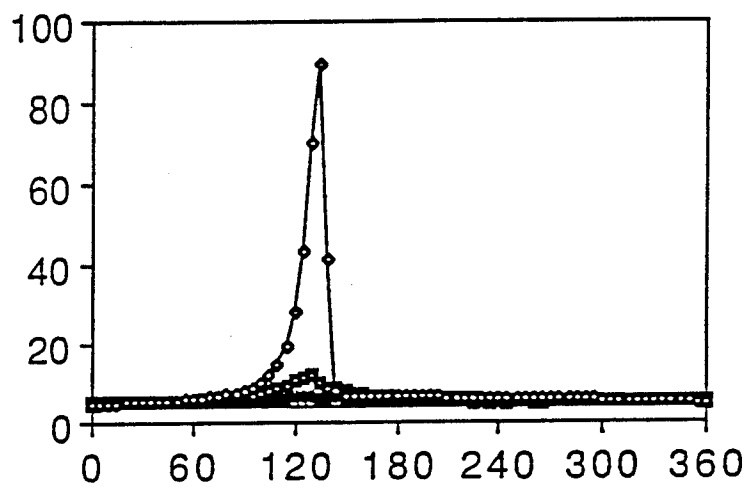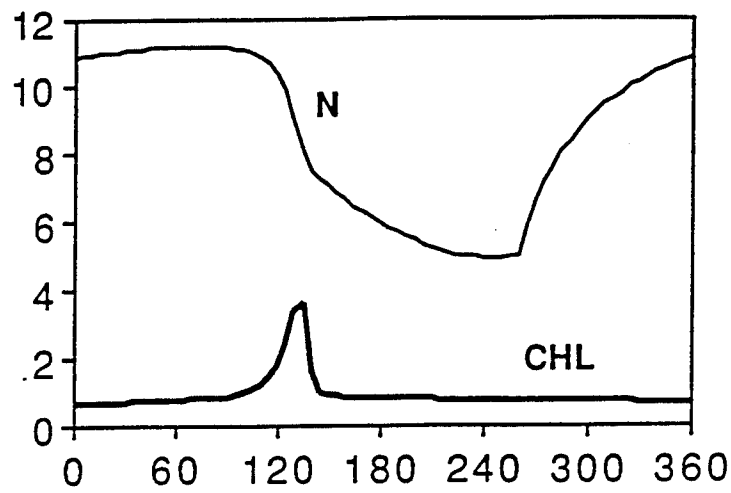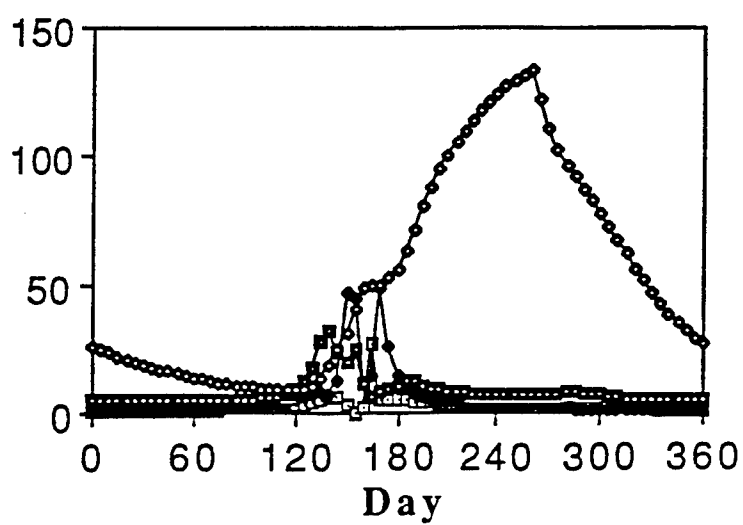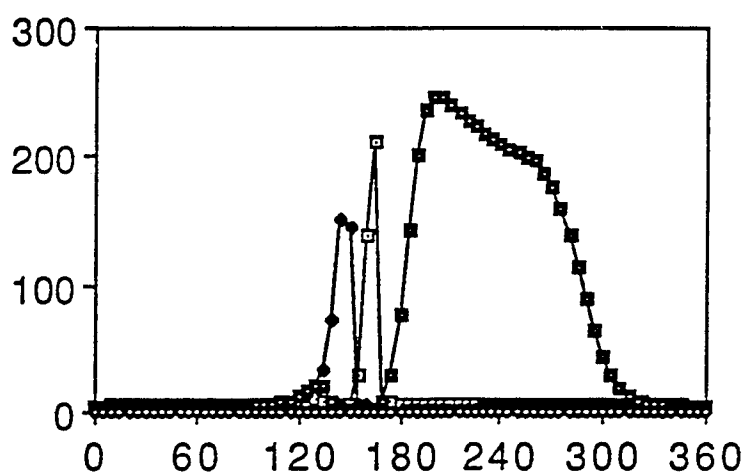
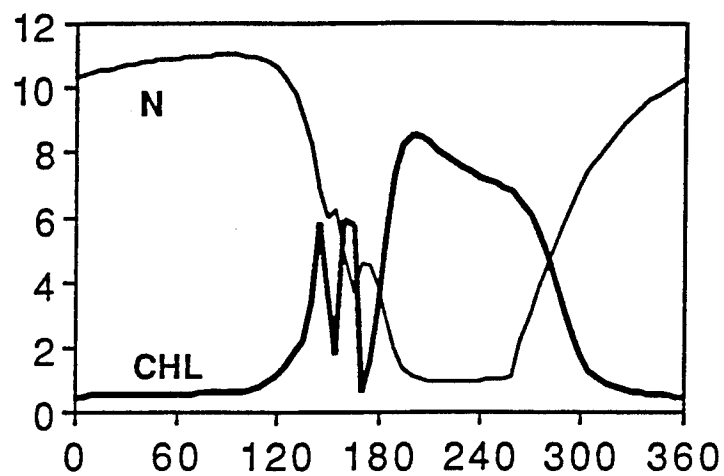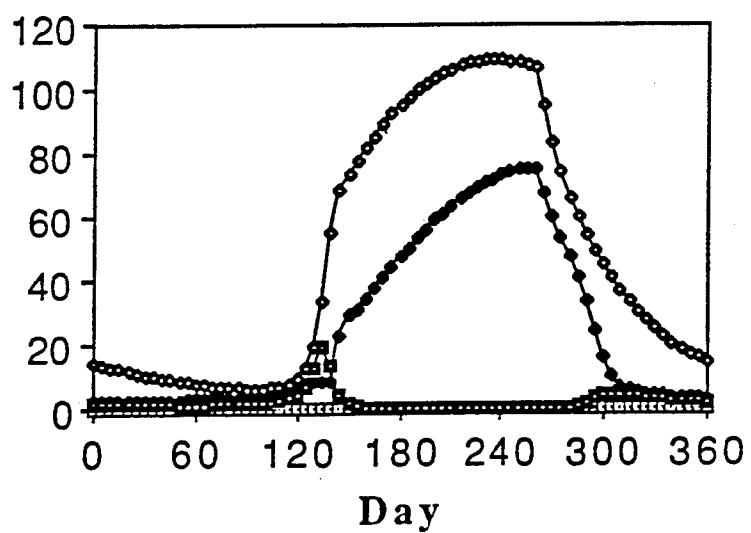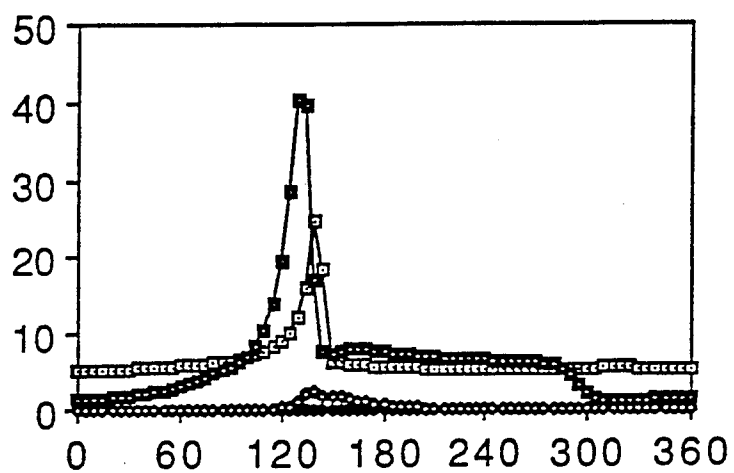Fig. 14. Model output using trophic structure 1.
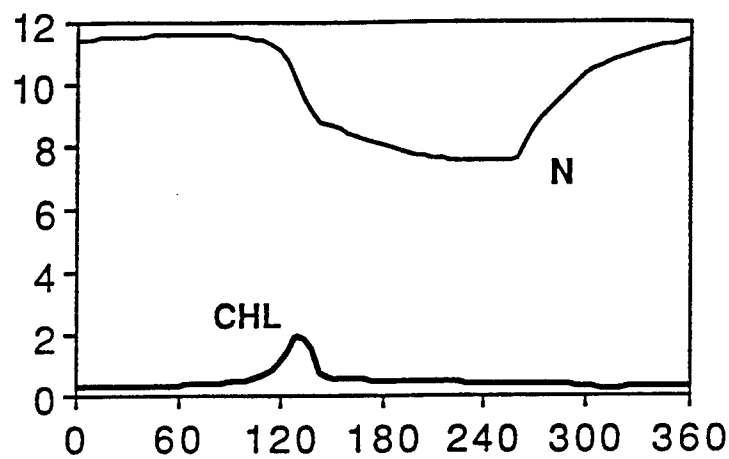
Fig. 15. Model output using trophic structure 2.

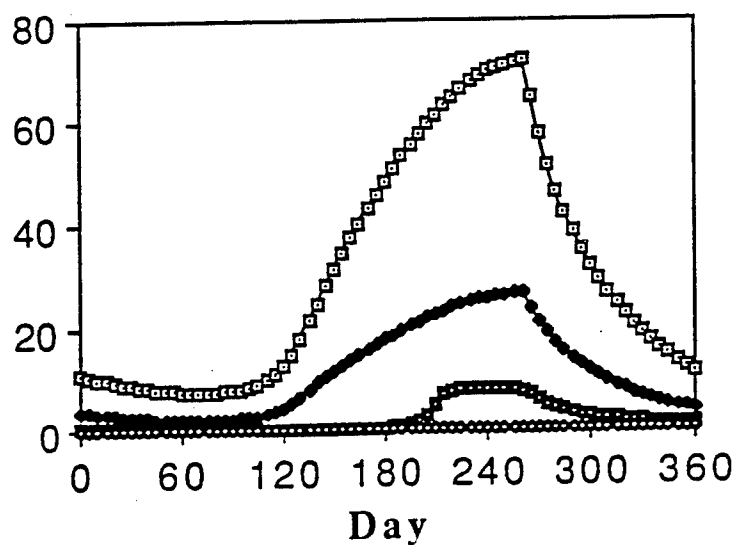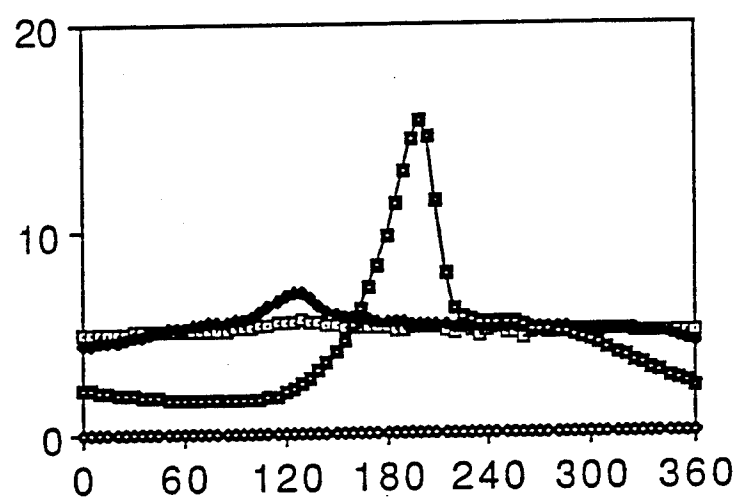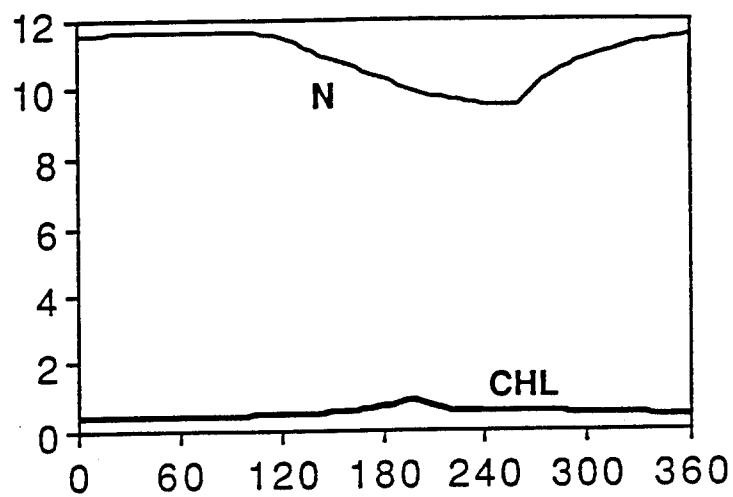Fig. 16. Model output using trophic structure 3.

Fig. 17. Model output using trophic structure 1 but with $\beta=-1.0$ for $\mu_{max,i}$. (Compare with Fig. 14).

33
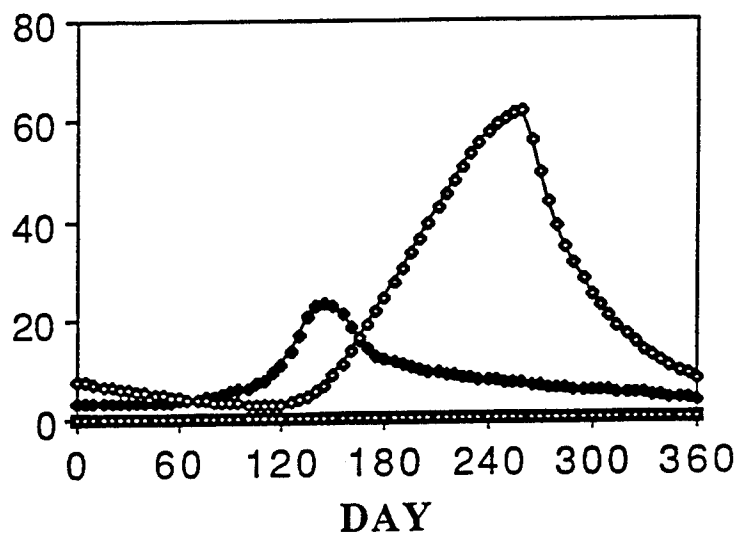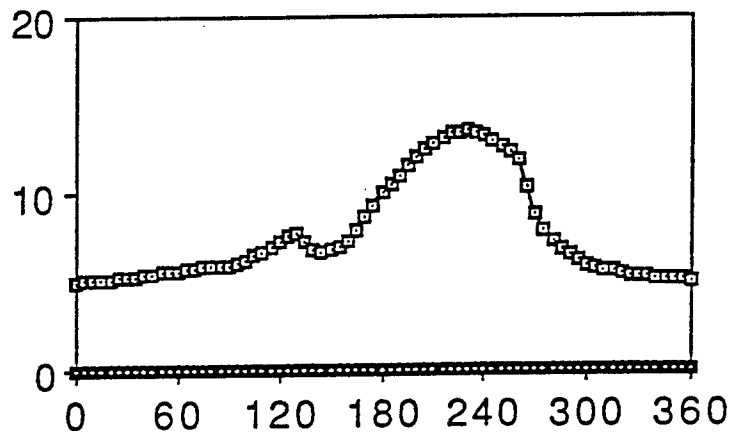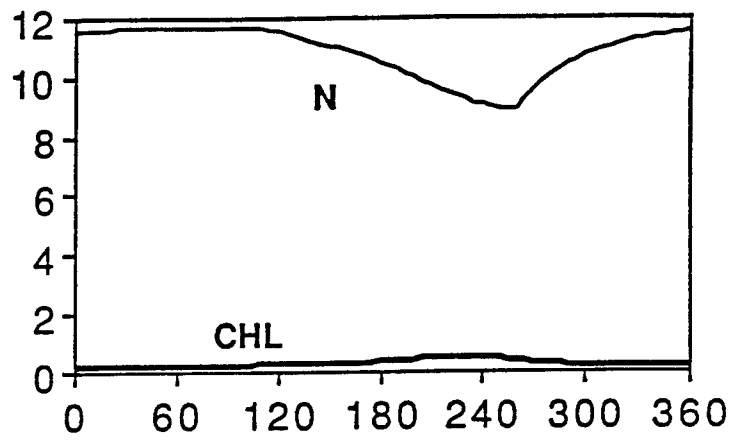
Fig. 18. Model output using trophic structure 4.

34

of P1 (not a feature observed in the open subarctic Pacific), with attendant depletion of N, but large sizes of phytoplankton still did not persist. The low chlorophyll-high N condition was recovered only by imposing heavy mortality on Z4.

Perhaps the most surprising outcome of these modelling studies was that introduction of trophic structure did not result inevitably in predicted annual cycles with blooms of large phytoplankton size classes. Indeed, predictions included "balanced" annual cycles and annual cycles with blooms of the smallest size class of phytoplankton. These few examples are sufficient to demonstrate that predictions of a food web model can be strongly influenced not only by the specific nature of the size-dependence of physiological processes modelled, but also by the trophic structure assumed, and the overall level of biological productivity. Knowledge of trophic interactions must be greatly improved before a particular trophic structure can be advocated in pelagic foodweb models for the open subarctic Pacific or other pelagic ecosystems.

### 3.3 Structured Populations

Davis, Olson (Chair), Pascual, Steele

### 3.3.1 Introduction

The idea of this working group is to explore means of taking structure in a population into account in coupled biological/physical models. Here structure can be defined as variations in individuals within a population which become expressed in terms of population density, $n$, changes in either space and/or time. The most general form can be expressed in terms of a conservation statement for the population which is expressed in an expansion of the total variation of $n$,

$$dn(t, s, w, \vec{x}) = \frac{\partial n}{\partial t}\, dt + \frac{\partial n}{\partial s}\, ds + \frac{\partial n}{\partial w}\, dw + \frac{\partial n}{\partial \vec{x}}\, d\vec{x} = -\mu n\, dt,$$

where the variables in the expansion are time ($t$), life-stage ($s$), body-weight ($w$), and space ($\vec{x}$). The $\mu$ term expresses mortality in the population. The total change in time of the population is then given by

$$\frac{dn}{dt} = \frac{\partial n}{\partial t} + \vec{v} \cdot \frac{\partial n}{\partial \vec{x}} + D^{-1}\frac{\partial n}{\partial s} + \hat{g}\frac{\partial n}{\partial w} = -\mu n.$$

Fluid dynamicists will recognize the material derivative in the first two partial expressions although here one might also include mobile behavior on the part of the population. The age or stage term gives the equation the form of McKendrick-von Foerster (McKendrick, 1926; von Foerster, 1959). In their case $D = 1$ and the dependence is on age. If the population has structure based on life stages which are not linear in time then $D$ becomes the stage duration function as discussed by Corkett and McLaren (1970) and McLaren (1978). The metabolic term is most commonly tied to the size or weight of the individual (Sinko and Streifer, 1967; de Roos et al., 1992). These choices of expansion variables are not unique. For example, the dependence of a population on its genetic structure might be considered (Webb, 1981). Finally, it is worth distinguishing the changes in the

properties of the equation if $\mu = \mu(n)$, *i.e.* the equation is nonlinear. Of coarse, it is assumed that in most cases $\mu$ will depend on the expansion variables, *c.f.* $\mu = \mu(s, w)$.

It is worthwhile commenting on the basic problem poised by the McKendrick-von Foerster equations and their method of solution. If for the moment interest is restricted to the case with $D = 1$ and ignoring the spatial terms the problem becomes

$$\partial n/\partial t + \partial n/\partial a = -\mu n.$$

This problem has both initial conditions, $n(a, 0) = n_o$, and a boundary condition based on reproduction in the population. The latter can be written in terms of an integral of a fecundity function $(F)$ over age,

$$n(0, t) = \int_0^\infty F(a, w, \gamma_F) \, da.$$

Here fecundity is assumed to be a function of age, physiological variables $(w)$, and an effective sex ratio for the population $(\gamma_F)$. Notice that the initial condition and the birth rate at $t = 0$ do not necessarily match. In this case the solution will have initial transients which must be solved for.

There are various means of seeking solutions to the McKendrick-von Foerster equation (*c.f.* Webb, 1985, Murray, 1989). For now consider the linear problem, $\mu \neq \mu(n)$. One of the most straight forward at least in concept is to introduce a cohort function for a population born at a given time, *i.e.* $n_c(t) = n(a_c + t)$ for $t \geq t_c$. The trajectory of the age of a cohort in time is a straight line as long as $D = 1$ and forms a characteristic for the solution for any $D$. The problem can then be solved for a individual cohort by integration along the characteristic as shown in Fig. 19. This solution for a given cohort is then

$$n_c(t) = n_c(t_c) exp[-\int_{t_c}^t \mu(t') \, dt'].$$

This can then be extended to an entire range of cohorts to given the general solution

$$n(a, t) = \begin{cases} n(0, t - a_c) exp[-\int_0^a \mu(t')dt], & t > a \\ n(a - t, 0) exp[-\int_{a-t}^a \mu(t')dt'], & t \leq a \end{cases}$$

For simple choices of $\mu$ these integrals can be solved. Another method for the long term limit on the population, $t >> a_{max}$, is to make use of similarity solutions of the form $n(a, t) = \hat{n}(a)e^{\gamma t}$. Upon substitution back into the original equation and some work on the birth condition this leads to viable solutions. Examples of similarity solutions are given by Murray (1989).

Our goal is to explore structured models in terms of some concrete examples for marine organisms and what they add to the dynamics of these populations. In particular the case of copepods with their multi-stage structured life-history will be considered. This report presents the basic copepod model formulated at the workshop. Then this basic model is embedded into an NPZ system. We briefly present directions to be pursued after the workshop.
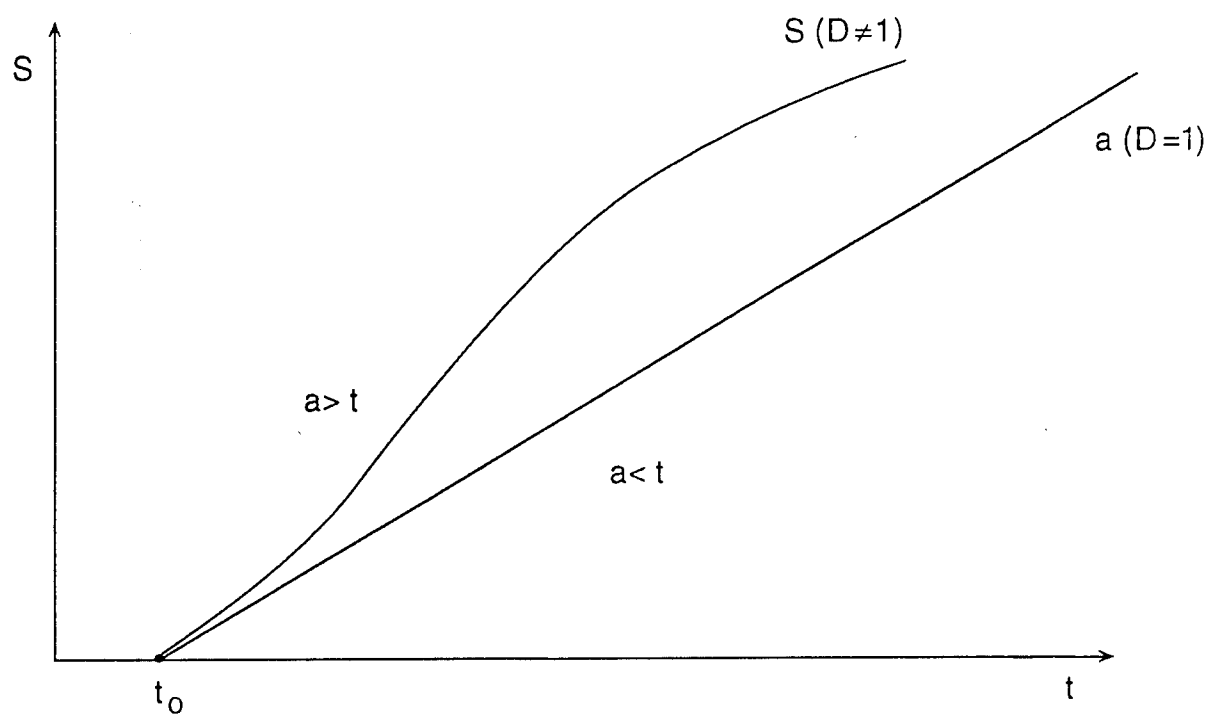
Fig. 19. Dependence of stage, $S$, upon time, $t$, for an organism born at time $t_0$. For a stage duration, $D = 1$, the organism is described by a linear age, $a$, function. For organisms such as crustaceans, which follow a pattern of descrete stages ($D \neq 1$), the stage curve will in general take some other form and fall to the left of the linear age relationship. See the text for further discusion.

### 3.3.2 *Basic copepod model*

We start by discretizing the cohorts such that there will be a separate equation for each cohort as identified by a subscript $i$. The model then, is based on three equations governing the weight of the average member of a cohort, the number of individuals in a cohort, and a diagnostic relationship for age/stage to time given a cohort's initial condition. For a general presentation of this approach see de Roos et al. (1992). The basic assumption made is a coupling between the mean condition of the cohort as governed by the mean weight, $w_i$, of the animals in a cohort of size $n_i$ through the influence of a consumption function, $f_i(P,T)$ where $P$ is a resource and $T$, the environmental temperature, and mortality, $m_i(w_i,T)$. General forms for these can be written as

$$\dot{w}_i = f_i(P,T)w_i$$

and

$$\dot{n}_i = -m_i(w_i,T)n_iw_i.$$

The basic problem then is to find appropriate forms for $m_i(w_i,T)$ and $f_i(P,T)$ and a relationship for the transition of the population through the stages which make up the life history of the organism.

As an example, consider a population of copepods which have growth curves as shown in Fig. 20. The ultimate growth rate is set by the exponential growth function of Huntley and Lopez (1992) for copepods. An individual species adapted to some region is assumed to have a more restricted growth function centered on some optimal temperature, $T_o$. The weight equation is then of the form

$$\dot{w}_i = R_oe^{\alpha_TT}exp\{-\beta(S)(T-T_o)^2\}(1-e^{-\lambda P})w_i$$

where the $(1-e^{-\lambda P})$ term is the Ivlev parameterization for resource limitation and $S$ is the stage of the copepod. The equation for the number of individuals in a cohort is given by

$$\dot{n}_i = -[m_o + m_1(w_o(S,t) - w_i(S,t))/w_o(S,t)]n_i$$

where $w_o$ is the optimal weight at stage for the species of interest. This optimal weight can be found by assuming food is not limiting, $P \to \infty$, and $T = T_o$. Under these assumptions

$$w_o = W_oexp\{R_oe^{\alpha_TT}t\}.$$

Finally, we need a relation for the stage of the copepod as a function of time. Here we take the stage duration ($D$) equation of form

$$D = a_i(T - \alpha_S)^b$$

after McLaren (1978). The stage of the copepod is then governed by the modulus of

$$S = S + dt/D(t)$$

38
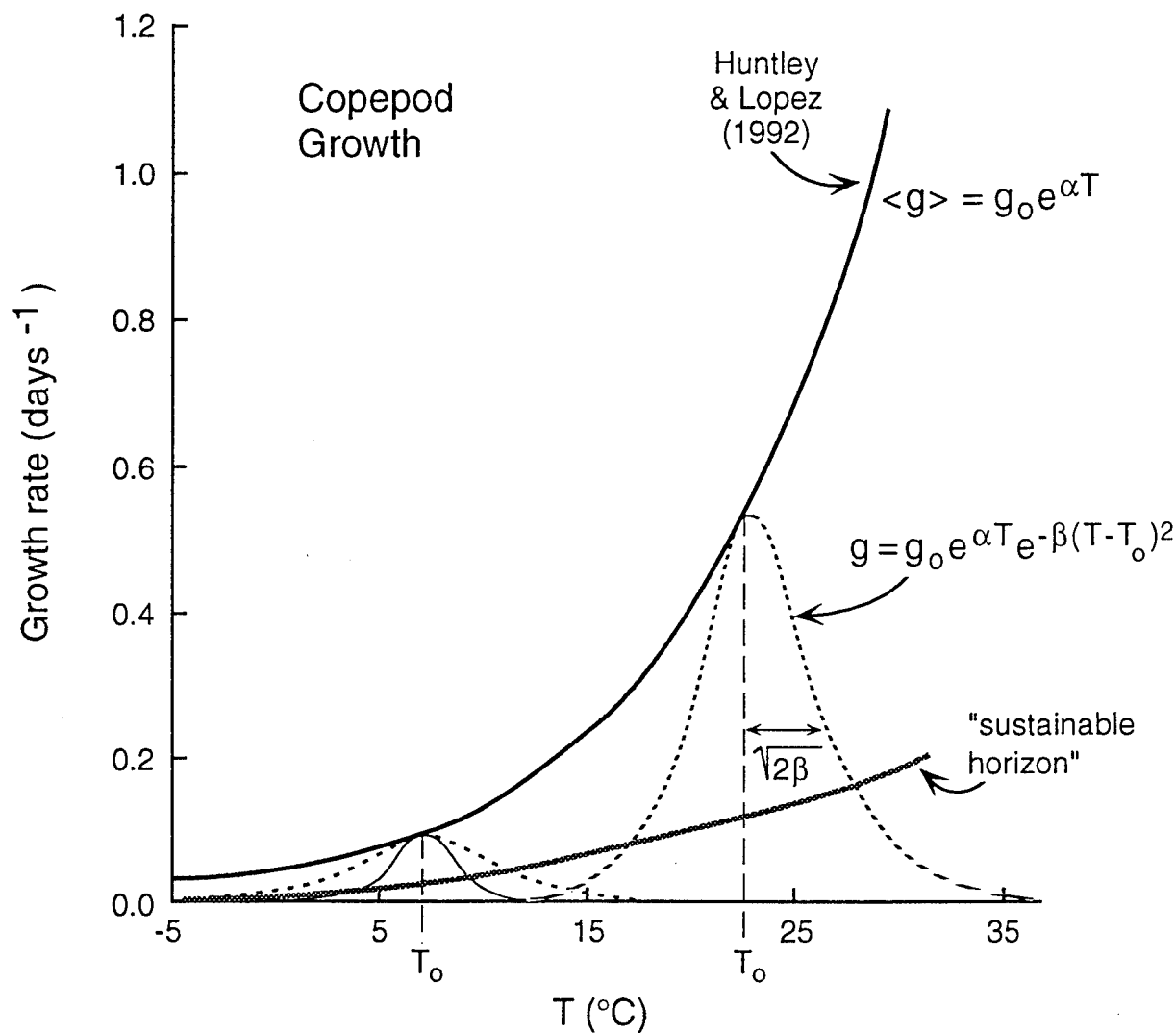
Fig. 20. Copepod growth as a function of environmental temperature. the solid curve is the exponential relationship found by Huntley and Lopez (1992) using a broad compilation of growth data. The dashed curves show the adaptive modification of this curve for copepods with an optimal temperature of $T_0$ and environmental range of half width $1/\sqrt{2\beta}$. A hypothetical limitation on growth rate is shown as a horizon below which the population becomes nonviable.

39

where $S$ has a value of one for eggs, 2-7 for naupliar stages I-VI, and 8-13 for the copepodid stages, the last stage, 13, being the adult copepod. We are applying these equations to the copepod *Calanus finmarchicus* and have also incorporated temperature-dependent diapause (a resting stage) in the fifth-stage copepodid.

### 3.3.3 *Coupling the model to the rest of the ecosystem*

The basic model in this work pictures a system consisting of nutrients, $N$, phytoplankton, $P$, and zooplankton, $Z$, where the latter is assumed to consist of a structured population. All of these variables have units of $[\mu mol/kg]$. A total population of zooplankton is divided into cohorts such that, $Z_T = \sum_i Z_i$, with $Z_i = n_i w_i$ where, as before, $w_i$ denotes the mean individual weight $[\mu mol/kg/individual]$, and $n_i$, the number of individuals of cohort $i$.

The total balance in the system is then governed by

$$\dot{N} = -aNP + \sum_i m_i(w_i, T) n_i w_i$$

$$\dot{P} = aNP - \sum_i f_i(P, T) n_i w_i$$

$$\dot{Z}_i = f_i(P, T) n_i w_i - m_i(w_i, T) n_i w_i$$

where the functions $m_i(w_i, T)$ and $f_i(P, T)$ denote the mortality and growth of the mean individual in each cohort.

We are investigating if and how incorporating structure modifies the dynamics of the NPZ system. We are presently considering the physical environment only through temporal forcing (i.e., the yearly temperature cycle and changes in light and nutrient supply as affected by changes in mixed layer depth). We plan to use this model in our ongoing biological-physical modeling studies which examine mixed-layer dynamics as well as two and three-dimensional circulations.

# 4. References

Armstrong, R.A. Grazing limitation and nutrient limitation in marine ecosystems: Steady-state solutions of an ecosystem model with multiple food chains. Limnol. Oceanogr. (in press)

Bleck, R., H. P. Hanson, D. Hu, and E. B. Kraus, 1989: Mixed layer–thermocline interaction in a three-dimensional isopycnic coordinate model, *J. Phys. Oceanogr.*, **19**: 1417-1439.

Booth, B.C. 1988. Size classes and major taxonomic groups of phytoplankton at two locations in the subarctic Pacific Ocean in May and August, 1984. Mar. Biol. 97:75-286.

Corkett, C. J. and McLaren, I. A. 1970. Relationships between development rate of eggs and older stages of copepods. *J. Mar. Biol. Assoc. U. K.*, **50**, 161-168.

Deardorff, J.W., 1972, Theoretical expression for the counter-gradient vertical heat flux, J. Geophys. Res., 77, 5900-5904.

de Roos, A. M., O. Diekmann, and J. A. J. Metz 1992. Studying the dynamics of structured population models: A versatile techniques and its application to *Daphnia. Amer. Natur.*, **139**, 123-147.

Fasham, M.J.R., J.L. Sarmiento, R.D. Slater, H.W. Ducklow, and R. William, 1993, Ecosystem behavior at Bermuda station "S" and ocean weather station "India": A general circulation model and observational analysis, Global Biogeochem. Cycles, 7(2), 379–415.

Flierl, G. R., and C. S. Davis, 1993: Biological effects of Gulf Stream meandering, *J. Mar. Res.*, in press.

Frost, B.W. 1987. Grazing control of phytoplankton stock in the open subarctic Pacific Ocean: a model assessing the role of mesozooplankton, particularly the large calanoid copepods, *Neocalanus* spp. Mar. Ecol. Prog. Ser. 39:49-68.

Huntley, M. E. and M. D. G. Lopez 1992. Temperature-dependent production of marine copepods: A global synthesis. *Amer. Natur.*, **140**, 201-242.

Large, W.G., J.C. McWilliams, and S.C. Doney, 1993, An ocean vertical mixing scheme with a K-profile boundary layer parameterization, submitted to Rev. Geophys.

Martin, J.H., R.M. Gordon, S.E. Fitzwater, and W.W. Broenkow. 1989. VERTEX: phytoplankton/iron studies in the Gulf of Alaska. Deep-Sea Res. 36:649-680.

McKendrick, A. G. 1926. Application of mathematics to medical problems. *Proc. Edinb. Math. Soc.*, **44**, 98-130.

McLaren, I. A. 1978. Generation lengths of some temperate marine copepods: Estimation, prediction and implications. *J. Fish. Res. Board Can.*, **35**, 1330-1342.

Miller, C.B., B.W. Frost, P.A. Wheeler, M.R. Landry, B.C. Booth, N. Welschmeyer, and T.M. Powell. 1991. Ecological dynamics in the subarctic Pacific, a possibly iron-limited ecosystem. Limnol. Oceanogr. 36:1600-1615.

Moloney, C.L., and J.G. Field. 1989. General allometric equations for rates of nutrient uptake, ingestion, and respiration in planktonic organisms. Limnol. Oceanogr. 34:1290-1299.

Moloney, C.L., and J.G. Field. 1991. The size-based dynamics of plankton food webs. I. A simulation model of carbon and nitrogen flows. J. Plankton Res. 13:1003-1038.

Murray, J. D. 1989. *Mathematical Biology*. Springer-Verlag, NY. 767pp.

Price, J. F., R. A. Weller, and R. Pinkel, 1986: Diurnal cycling: Observations and models of the upper ocean response to diurnal heating, cooling, and wind mixing, *J. Geophys. Res.*, **91**: 8411-8427.

Sinko, J. W. and W. Streifer 1967. A new model for age-size structure of a population. *Ecology*, **48**, 910-918.

Smith, S.D. and F.W. Dobson, 1984, The heat budget at Ocean Weather Station Bravo, Atmos.-Oceans, 22, 1-22.

Webb, G. 1981. A genetics model with age dependence and spatial diffusion. In *Differential Equations and Applications in Ecology, Epidemics, and Population Problems.*, XXXXX (ed), Acad. Press, Inc., 29-29. Webb, G. 1985. *Theory of Nonlinear Age-Dependent Population Dynamics*, York: Marcel Dekker, Inc. 294 pp.

von Foerster, H. 1959. Some remarks on changing populations. *in The Kinematics of Cellular Proliferation.*, F. Stohlman, Jr. (ed.), Grune and Stratton, New York, 382-407.

# Appendix I. List of participants

## URIP MODELING WORKSHOP
### JUNE 7-12, 1993

| NAME | ADDRESS | TELEPHONE/EMAIL |
|------|---------|-----------------|
| Archer, David | Department of Geophysical Sciences<br>5734 S. Ellis Ave.<br>University of Chicago<br>Chicago, Ill 60637 | (312) 702 0823<br>archer@popeye.uchicago.edu |
| Armstrong, Robert | Atmospheric and Oceanic Sciences Program<br>Sayre Hall, P.O. Box CN710<br>Princeton University<br>Princeton, NJ 08544-0710 | (609) 258-5260<br>raa@splash.princeton.edu |
| Bollens, Steve | W.H.O.I.<br>Redfield 2-44<br>Woods Hole, MA 02543 | (508) 457-2000 x3213<br>sbollens@whoi.edu |
| Caron, David | W.H.O.I.<br>Redfield 3-24<br>Woods Hole, MA 02543 | (508) 457-2000 x2358<br>D.CARON (OMNET) |
| Caswell, Hal | W.H.O.I.<br>Redfield 1-04<br>Woods Hole, MA 02543 | (508) 457-2000 x2751<br>hcaswell@whoi.edu |
| Changsheng, Chen | Dept. of Oceanography<br>Texas A&M University<br>College Station, TX 77843 | (409) 862-4168<br>chen@latexa.tamu.edu |
| Davis, Cabell | W.H.O.I.<br>Redfield 2-22<br>Woods Hole, MA 02543 | (508) 457-2000 x2333<br>davis@plankton.whoi.edu |
| Denman, Kenneth | Inst. of Ocean Sciences<br>Fisheries and Oceans<br>P.O. Box 6000<br>9860 W. Saanich Road<br>Sidney, B.C. Canada V8L 4B2 | (604) 363-6346<br>denman@ios.bc.ca<br>K.DENMAN (OMNET) |
| Doney, Scott | NCAR<br>Advanced Study Program<br>P.O. Box 3000<br>Boulder, CO 80307 | (303) 497-1639<br>doney@ncar.ucar.edu |

| NAME | ADDRESS | TELEPHONE/EMAIL |
|------|---------|-----------------|
| Flierl, Glenn | MIT<br>Earth Atmosphere &<br>Planetary Sciences<br>Cambridge, MA 02139 | (617) 253-4692<br>glenn@lake.mit.edu |
| Franks, Peter | Marine Life Research Group<br>Scripps Institution of<br>Oceanography 0218<br>Univ. of Calif., San Diego<br>LaJolla, CA 92093 | (619) 534-7528<br>franks@ucsd.edu |
| Frost, Bruce | College of Ocean<br>Fishery Science<br>304 Marine Sciences<br>Bldg., WP-10<br>Univ. of Washington<br>Seattle, WA 98195 | (206) 543-7186<br>B.FROST (OMNET) |
| Gawarkiewicz, Glen | W.H.O.I.<br>Clark 3-44<br>Woods Hole, MA 02543 | (508) 457-2000 x2913<br>glen@paddle.whoi.edu |
| Glover, David | W.H.O.I.<br>Clark 4-25<br>Woods Hole, MA 02543 | (508) 457-2000 x2656<br>david@plaid.whoi.edu |
| Hood, Raleigh | Univ. of Miami<br>RSMAS<br>4600 Rickenbacker<br>Causeway<br>Miami, FL 33149 | (305) 361-4108<br>raleigh@mango.rsmas.miami.edu |
| Landry, Michael | Department of Oceanography<br>Univ. of Hawaii at Manoa<br>1000 Pope Road, MSB 307<br>Honolulu, HI 96822 | (808) 956-7776<br>M.LANDRY (OMNET) |
| Landsteiner, Mary | Oceanography WB-10<br>Univ. of Washington<br>Seattle, WA 98195 | (206) 543-3358<br>maryland@ocean.washington.edu |
| Levin, Simon | Dept. of Ecology and<br>Evolutionary Biology<br>Eno Hall - Princeton Univ.<br>Princeton, NJ 08544-1003 | (609) 258-5880<br>simon@pac0.princeton.edu |

| NAME | ADDRESS | TELEPHONE/EMAIL |
|------|---------|-----------------|
| Lewis, Craig | W.H.O.I.<br>Redfield 2-22<br>Woods Hole, MA 02543 | (508) 457-2000 x4814<br>cvl@skellam.whoi.edu |
| Little, Sarah | W.H.O.I.<br>Redfield 1-14<br>Woods Hole, MA 02543 | (508) 457-2000 x3245<br>slittle@attractor.whoi.edu |
| Moisan, John | Scripps Inst. Oceanography<br>Physical Oceanography Res.<br>Division<br>9500 Gilman Drive<br>LaJolla, CA 92093-0230 | (619) 534-7153<br>moisan@drifter.ucsd.edu |
| Olson, Donald | RSMAS<br>4600 Rickenbacker<br>Causeway<br>Miami, FL 33149 | (305) 361-4074<br>don@miami.rsmas.miami.edu<br>D.OLSON.RSMAS (OMNET) |
| Sarmiento, Jorge | Princeton University<br>AOS Program<br>Princeton University<br>P.O. Box CN710<br>Princeton, NJ 08544-0710 | (609) 258-6585<br>jls@phoenix.princeton.edu<br>J.SARMIENTO (OMNET) |
| Steele, John | W.H.O.I.<br>Crowell House<br>Woods Hole, MA 02543 | (508) 457-2000 x2220<br>jsteele@whoi.edu<br>J.STEELE (OMNET) |

# Appendix II. References to existing mixed-layer models
Provided by: David Archer, University of Chicago

Adamec, D., Elsberry, R.L., Garwood, R.W., Haney, R.L. 1981. An embedded mixed-layer – ocean circulation model. *Dyn. Atmos. Oceans*, **6**, 69-96.
*Keywords* – upper ocean, mixed layer, OGCM, embedded mixed layer, commented, and DOE
*Description* – They formulate an embedded DIM (a la Price, Weller, Pinkle) using only the gradient Ri instability (no bulk Ri). Below the Ri zone, they use K's of 0.5 cm2/s. See also Garwood, 77; Haney, 85; and Pacanowski and Philander, 81; Niiler, 75; DeSzoeke, 76.

Adamec, D., Garwood, R.W.Jr. 1985. The simulated response of an upper-ocean density front to local atmospheric forcing. *J. Geophys. Res.*, **90(C1)**, 917-928.
*Keywords* – upper ocean, OGCM, Ri formulation, horizontal heterogeneity, mixed layer, and commented
*Description* – Uses the model from Adamec et al., 1981, which comes from Garwood, 77, a partially Ri dependent mixing model.

Alexander, R.C., Kim, J-.W. 1976. Diagnostic model study of mixed-layer depths in the summer North Pacific. *J. Phys. Ocean.*, **6**, 293-298.
*Keywords* – upper ocean, mixed layer, 1D, bulk model, wind stress scaling, and commented
*Description* – They present a different parameterization of the dissipation term, to fit data in the North Pacific.

Briscoe, M.G., Weller, R.A. 1984. Preliminary results from the long-term upper-ocean study (LOTUS). *Dyn. Atmos. Oceans*, **8**, 243-265.
*Keywords* – upper ocean, internal waves, mixed layer, 1D, and data

Davis, R.E., deSzoeke, R., Niiler, P. 1981. Variability in the upper ocean during MILE. Part I: The heat and momentum balances. *Deep Sea Res.*, **28A(12)**, 1427-1451.
*Keywords* – upper ocean, mixed layer, 1D, data, and DOE

Davis, R.E., dsSzoeke, R., Niiler, P. 1981. Variability in the upper ocean during MILE. Part II: Modeling the mixed layer response. *Deep Sea Res.*, **28A(12)**, 1453-1475.
*Keywords* – upper ocean, mixed layer, 1D, bulk model, Ri formulation, wind stress scaling, commented, and DOE
*Description* – They find that both types of turbulence production, shear and wind, are needed to simulate their data from part I. of the set, but are dubious about interpreting this as evidence of understanding the mechanism involved. They also find that it's important to allow solar heating to happen as a function of depth; in the summer, lots of heating happens below the surface.

Deardorff, J.W. 1983. A multi-limit mixed layer entrainment formulation. *J. Phys. Ocean.*, **13**, 988-1002.

*Keywords* – upper ocean, mixed layer, 1D, turbulence closure, Ri formulation, and commented
*Description* – A "second order" differential model, for which the model entrainment rate has been evaluated as a function of various Ri's. He also compares the formulations (wind, current).

Denman, K.L. 1973. A time-dependent model of the upper ocean. *J. Phys. Ocean.*, **3**, 173-184.
*Keywords* – upper ocean, mixed layer, 1D, bulk model, wind stress scaling, and commented
*Description* – Cites Kato and Phillips (69) as evidence that surface-produced turbulence (as opposed to shear) drives the mixed layer. (See deSzoeke and Rhines, 1976; Kitaigorodskii, 1981, for further discussion on this point). A somewhat more rigorous derivation and explanation of the KT model.

Denman, K.L., Miyake, M. 1973. Upper ocean modification at Ocean Station Papa: observations and simulation. *J. Phys. Ocean.*, **3**, 185-196.
*Keywords* – upper ocean, mixed layer, 1D, data, and commented
*Description* – Goes with Denman, 73.

deSzoeke, R.A., Rhines, P.B. 1976. Asymtotic regimes in mixed-layer deepening. *J. Mar. Res.*, **34**, 111-116.
*Keywords* – upper ocean, mixed layer, 1D, bulk model, Ri formulation, wind stress scaling, and commented
*Description* – Mathematical argument that the wind stress scaling ought to only hold for the initial part of the spin-up, then the shear part ought to take over.

Dillon, T.M., Richman, J.G., Hansen, C.G., Pearson, M.D. 1981. Near surface turbulence measurements in a lake. *Nature*, **290**, 390-392.
*Keywords* – upper ocean, turbulence, dissipation, and mixed layer

Elsberry, R.L., Friam, T.S., Trapnell, R.N.Jr. 1976. A mixed layer model of the oceanic thermal response to hurricanes. *J. Geophys. Res.*, **81(6)**, 1153-1162.
*Keywords* – upper ocean, mixed layer, 1D, bulk model, wind stress scaling, commented, and DOE
*Description* – They use a KT type model, with a new parameterization of the dissipation term.

Gargett, A.E., Sanford, T.B., Osborn, T.R. 1979. Surface mixing layers in the Sargasso Sea. *J. Phys. Ocean.*, **9**, 1090-1111.
*Keywords* – upper ocean, mixed layer, 1D, turbulence, Ri formulation, commented, and DOE
*Description* – They suggest that, based on their microstructure measurements during a couple of storms, the deepening occurred as a result of shear, rather than wind. Also, the budget of TKE was not always in balance; the dq/dt term was nonzero.

Garwood, R.W. 1977. An ocean mixed layer model capable of simulating cyclic states. *J. Phys. Ocean.*, **7**, 455-468.

*Keywords* – upper ocean, mixed layer, 1D, bulk model, Ri formulation, commented, and DOE

*Description* – Addresses the bulk Ri formulation of Pollard et al. on page 459. Contrasts the other formulations. The models of Adamec were based on this model. Uses both the Ri and the wind stress scaled mixing, but concludes that the Ri mixing is unimportant. Sort of a hybrid model.

Gaspar, P. 1988. Modeling the seasonal cycle of the upper ocean. *J. Phys. Ocean.*, **18**, 161-180.

*Keywords* – upper ocean, mixed layer, 1D, bulk model, wind stress scaling, commented, and DOE

*Description* – A bulk wind-stress scaled mixed layer model with an improved dissipation term.

Gaspar, P., Gregoris, Y., Lefevre, J.M. 1990. A simple eddy kinetic energy model for simulations of the oceanic vertical mixing: tests at station papa and the long-term upper ocean study site. *J. Geophys. Res.*, **95**, 16179-193.

*Keywords* – upper ocean, mixed layer, 1d, thermocline, diapycnal mixing, and papa

Gill, A.E., Turner, J.S. 1976. A comparison of seasonal thermocline models with observation. *Deep Sea Res.*, **23**, 391-401.

*Keywords* – upper ocean, mixed layer, 1D, bulk model, wind stress scaling, and DOE

Han, Y.J. 1984. A numerical world ocean general circulation model Part II. A baroclinic experiment. *Dyn. Atm. Oceans*, **8**, 141-172.

*Keywords* – upper ocean, OGCM, climate model, OSU, mixed layer, and commented

*Description* – In Part I. of this set, he says that he uses the mixed layer parameterization by Kim and Gates (1980), an OSU technical report. This equation doesn't look like the formula in the DOE report. He also uses the sea ice formulation by Parkinson and Washington (79), which is a solid ice heat flux model based on Semtner (76). Heat fluxes are predicted using air temp, wind speed, etc., also mom fluxes.

Han, Y.J., Gates, W.L. 1989. A new surface mixed alyer and sea-ice parameterization. *From an NSF proposal*, Appendix 1.

*Keywords* – upper ocean, mixed layer, OGCM, and commented

*Description* – Description of their embedded mixed layer formulation.

Haney, R.L., Davies, R.W. 1976. The role of surface mixing in the seasonal variation of the ocean thermal structure. *J. Phys. Ocean.*, **6**, 504-510.

*Keywords* – upper ocean, mixed layer, 1D, bulk model, wind stress formulation, and commented

*Description* – A very simple model such as used in GCM's. Anything new?

Haney, R.L. 1985. Midlatitude sea surface temperature anamolies: a numerical hindcast. *J. Phys. Ocean.*, **15**, 787-799.

*Keywords* – upper ocean, OGCM, SST, mixed layer, Ri formulation, and commented

*Description* – Pacific region model. 12 depth levels above 200 m. Surface mixing is done using a gradient Ri formulation, with critical value 0.25. Follows Adamec, 1981. Heat fluxes calculated from bulk formulae. Tries to predict the SST anomalies associated with ENSO, and is partially successful.

Holland, W.R. 1977. The role of the upper ocean as a boundary layer in models of the oceanic general circulation. In: *Modelling and Prediction of the Upper Layers of the Ocean*, Kraus (Ed.), Pergammon Press, Oxford, 7-29.

*Keywords* – upper ocean, mixed layer, OGCM, and commented

*Description* – Discusses, among other things, the KT mixed layer in Bryan (75) and Manabe (75) (coupled papers).

Hughes, R.L. 1980. On the equatorial mixed layer. *Deep Sea Res.*, **27A**, 1067-1078.

*Keywords* – upper ocean, mixed layer, 1D, equatorial ocean, OGCM, and commented

*Description* – Referenced by Pacanowski and Philander (81). Equatorial mixed layer model using KT formulation. P&P claim that this model lacks the "horizontal redistribution of heat" that they claim is essential to explain the equatorial mixed layer. Hughes claims that Bryan and Cox (68) find that in the equator, only vertical processes are important.

Kamenkovich, V.M., Khar'kov, B.V. 1975. On the seasonal variation of the thermal structure of the upper layer in the ocean. *Oceanology*, **15**, 642-647.

*Keywords* – upper ocean, mixed layer, 1D, bulk model, wind stress scaling, and DOE

Kantha, L.H. 1977. Note on the role of internal waves in thermocline erosion. In: *Modelling and Prediction of the Upper Layers of the Ocean*, Kraus (Ed.), Pergammon Press, Oxford, 1773-177.

*Keywords* – upper ocean, turbulence, internal waves, and mixed layer, 1D

Kato, H., Phillips, O.M. 1969. On the penetration of a turbulent layer into stratified fluid. *J. Fluid Mech.*, **37** (4), 643-655.

*Keywords* – upper ocean, mixed layer, bulk model, physical basis, and commented

*Description* – See also deSzoeke and Rhines 76, and Kitaigorodskii 81.

Kessler, T.A.. Oxygen production and nitrate uptake estimates from the heat, oxygen, and nitrate budgets at station Papa: evidence of seasonal trophic changes in the subarctic Pacific. (in draft).

*Keywords* – upper ocean, mixed layer, 1D, new production, biology, and dissolved oxygen

*Description* – He gets new production rates at Papa of 50-100 gC/m2y (O2 supersat method) and 10-60 gC/m2y (NO3 consumption method).

Kim, J-.W. 1976. A generalized bulk model of the oceanic mixed layer. *J. Phys. Ocean.*, **6**, 686-695.

*Keywords* – upper ocean, mixed layer, 1D, bulk model, wind stress scaling, commented, and DOE

*Description* – Related to the mixed layer embedded model in OSU's GCM?

Kitaigorodskii, S.A. 1981. On the theory of the surface-stress induced entrainment at a buoyancy interface (toward interpretation of KP and KPA experiments). *Tellus*, **33**, 89-101.

*Keywords* – upper ocean, mixed layer, 1D, bulk models, model comparison, Ri formulation, wind stress scaling, physical basis, commented, and DOE

*Description* – Attempts to reconcile the data of Kato and Phillips (69) with shear-generated turbulence ideas. See also deSzoeke and Rhines, 76.

Klein, P., Coantic, M. 1981. A numerical study of turbulent processes in the marine upper layers. *J. Phys. Ocean.*, **11**, 849-863.

*Keywords* – upper ocean, mixed layer, 1D, turbulence closure, commented, and DOE

*Description* – They use Mellor's L3 model. They find that deepening occurs due to the shear, rather than by the wind directly.

Klein, P., Coste, B. 1984. Effects of wind-stress variability on nutrient transport into the mixed layer. *Deep Sea Res.*, **31(1)**, 21-37.

*Keywords* – upper ocean, mixed layer, 1D, turbulence closure, new production, flux across thermocline, and commented

*Description* – They use Mellor's L2 model, and find that mixing occurs due to shear, rather then directly by the wind. They find that nuts mix up in pulses, rather than steadily.

Kraus, E.B., Turner, J.S. 1967. A one-dimensional model of the seasonal thermocline II. The general theory and its consequences. *Tellus*, **19**, 98-105.

*Keywords* – upper ocean, mixed layer, 1D, bulk model, wind stress scaling, commented, and DOE

*Description* – The classic. Later improvements were made in the dissipation term (many authors).

Kroll, J. 1988. Instability of a mixed later model and the generation of near-inertial motion. Part I: Constant mixed layer depth. *J. Phys. Ocean.*, **July**, 963.

*Keywords* – upper ocean, mixed layer, and near inertial motions

Martin, P.J. 1985. Simulation of the mixed layer at OWS November and Papa with several models. *J. Geophys. Res.*, **90(C1)**, 903-916.

*Keywords* – upper ocean, mixed layer, model comparison, commented, and DOE

*Description* – See the technical report.

Martin, P.J. 1986. Testing and comparison of several mixed-layer models. *Naval Ocean Research and Development Activity Tech Rep*, **143**.

*Keywords* – upper ocean, mixed layer, model comparison, commented, and DOE

*Description* – Gives computer costs, memory constraints, and how well the models simulate the observed data, both on long and short time scales. 1) Data from

FLIP in PWP not well simulated by the turbulence closure models – they must not mix in the mixed layer by the complete mechanism. 2) KT models have that disturbing "jump" at the base of the mixed layer. 3) The various turbulence closure models only differ in their Ri-crit for mixing. They are mostly shear models, due to low turbulence transport in the models.

Meehl, G.A., Washington, W.M. 1985. Sea surface temperatures computed by a simple ocean mixed layer coupled to an atmospheric GCM. *J. Phys. Ocean.*, **15**, 92-104.
*Keywords* – upper ocean, AGCM, coupled A-O, SST, NCAR, and with slab mixed layer
*Description* – Atmos. GCM with a slab ocean mixed layer. They find that the SST is fairly well represented most places, but to high in eq. upwelling areas (no advection in ocean). Mixed layer is of a fixed depth, 50m.

Mellor, G.L. 1973. Analytic prediction of the properties of stratified planetary surface layers. *J. Atm. Sci.*, **30**, 1061-1069.
*Keywords* – upper ocean, mixed layer, 1D, TKE model, commented, and DOE
*Description* – One of the originals

Mellor, G.L., Yamada, T. 1974. A hierarchy of turbulence closure models for planetary boundary layers. *J. Atmos. Sci.*, **31**, 1791-1806.
*Keywords* – upper ocean, mixed layer, 1D, turbulence closure, commented, and DOE
*Description* – Adds the simplification scheme to get all the different levels of models.

Mellor, G.L., Durbin, P.A. 1975. The structure and dynamics of the ocean surface mixed layer. *J. Phys. Ocean.*, **5**, 718-728.
*Keywords* – upper ocean, mixed layer, 1D, turbulence closure, commented, and DOE
*Description* – "Comparisons of predictions and data are favorable."

Mellor, G.L. 1979. Retrospective on oceanic boundary layer modeling and second moment closure, (in manuscript).
*Keywords* – upper ocean, mixed layer, 1D, turbulence closure, commented, and DOE
*Description* – Another summary of the physics, reflecting recent discussion in the field.

Mellor, G.L., Yamada, T. 1982. Development of turbulence closure model for geophysical fluid problems. *Rev. Geophys. Space Phys.*, **20(4)**, 851-875.
*Keywords* – upper ocean, mixed layer, 1D, turbulence closure, commented, and DOE
*Description* – And away we go.

Miyakoda, K., Rosati, A. 1984. The variation of sea surface temperature in 1976 and 1977 2. The simulation with mixed layer models. *J. Geophys. Res.*, **89(C4)**, 6533-6542.

*Keywords* – upper ocean, mixed layer, 1D, model comparison, bulk model, wind stress scaling, turbulence closure, and commented

*Description* – They spread out 1D mixed layer models over the Pacific to figure out why the temperatures were anomalous during 1977. No transport (1 by N model, like Glover's). Found that both types under-mixed the water between surface and deep, and concluded that Mellor level 2.0 was not good enough. Concluded, like Rosatti (8X) that monthly mean wind data is not good enough.

Moum, J.N., Caldwell, D.R., Paulson, C.A. 1989. Mixing in the equatorial surface layer and thermocline. *J. Geophys. Res.*, **94 (C2)**, 2005-2023.
*Keywords* – upper ocean, equatorial ocean, mixed layer, turbulence, and dissipation

Musgrave, D.L., Chou, J., Jenkins, W.J. 1988. Application of a model of upper-ocean physics for studying seasonal cycles of oxygen. *J. Geophys. Res.*, **93**, 15679-15700.
*Keywords* – upper ocean, mixed layer, 1D, new production, dissolved oxygen, bulk model, Ri formulation, commented, and DOE
*Description* – Gets new production rates of 3-4 mol O2/m2y, which is about 32 gC/m2y, as opposed to 50 (from Jenkins and Goldman, 85). Paper also interesting in that he had to put in a diffusivity to get the annual SST cycle right. P.Martin didn't have to do that.

Niiler, P.P., Kraus, E.B. 1977. One-dimensional models of the upper ocean. In: *Modelling and Prediction of the Upper Layers of the Ocean*, Kraus (Ed.), Pergammon Press, Oxford, 143-172.
*Keywords* – upper ocean, mixed layer, 1D, bulk model, wind stress scaling, commented, and DOE
*Description* – The original.

Pacanowski, R.C., Philander, S.G.H. 1981. Parameterization of vertical mixing in numerical models of tropical oceans. *J. Phys. Ocean.*, **11**, 1443-1451.
*Keywords* – upper ocean, mixed layer, thermocline ventilation, OGCM, Ri formulation, commented, and DOE
*Description* – Outline a Ri-dependent eddy mixing formulation. These vary continuously with Ri, rather than being turned on at a critical Ri, as in PWP. Also, they are gradient Ri's, not bulk Ri's. PWP was unable to make his model work with just Ri(grad). Perhaps the difference is the lower resolution of this model (5 boxes in upper 100m).

Phillips, O.M. 1966. *The dynamics of the upper ocean*, Cambridge Press, London.
*Keywords* – upper ocean, fluid mechanics, turbulence, mixed layer, and DOE

Pollard, R.T., Rhines, P.B., Thompson, R.O.R.Y. 1973. The deepening of the wind-mixed layer. *Geophys. Fluid Dyn.*, **3**, 381-404.
*Keywords* – upper ocean, mixed layer, 1D, bulk model, Ri formulation, physical basis, commented, and DOE

*Description* – Elegant paper, laying out lots of reasons why the bulk Ri formulation is more correct than the wind stress scaling. See also deSzoeke and Rhines, 76.

Pollard, R.T., Thomas, K.J.H. 1989. Vertical circulation revealed by diurnal heating of the upper ocean in late winter, part I: observations. *J. Phys. Ocean.*, **19**, 269.
*Keywords* – upper ocean, mixed layer, convective mixing, data, and commented
*Description* – They observe convective mixing in the surface ocean.

Price, J.F., Mooers, C.N.K., Van, Leer. 1978. Observations and simulation of storm-induced mixed-layer deepening. *J. Phys. Ocean.*, **8**, 582-599.
*Keywords* – upper ocean, mixed layer, 1D, bulk model, model comparison, Ri formulation, wind stress scaling, commented, and DOE
*Description* – Argues strongly that the Ri scaling is superior to the wind scaling, with some observations and comparisons with the model. Finds that the empirical constants needed for wind scaling change under different conditions, whereas for the Ri scaling, they are pretty constant.

Price, J.F., Weller, R.A., Pinkle, R. 1986. Diurnal cycling: observations and models of the upper ocean response to diurnal heating, cooling and wind mixing. *J. Geophys. Res.*, **91(C7)**, 8411-8427.
*Keywords* – upper ocean, mixed layer, 1D, bulk model, Ri formulation, commented, and DOE
*Description* – The new classic Ri model, with the innovation of the smoothing of the base of the mixed layer using a Ri-gradient formulation, which slows it down but gives a more realistic water column profile (see Martin's technical report). Also some great high-resolution diurnal mixed layer current meter and CTD data from FLIP, which shows higher mixing in the "mixed" layer than is predicted by the turbulence closure models (see again Martin).

Rosati, A., Miyakoda, K. 1988. A general circulation model for upper ocean simulation. *J. Phys. Ocean.*, **18**, 1601-1626.
*Keywords* – upper ocean, mixed layer, OGCM, Princeton - GFDL, turbulence closure, commented, and DOE
*Description* – OGCM skewed toward upper ocean detail. 6 levels in upper 70m. Mellor level 2.5 turbulence closure. 12-hr average winds worked better than monthly averages (evap heat flux underestimated with monthly ave.). Heat fluxes calculated using bulk formulae. No mention of sea ice.

Sarachik, E.S. 1978. Boundary layers on both sides of the tropical ocean surface. In: *The Global Weather Experiment: FINE workshop proceedings*, Nova / N.Y.I.T. Univ. Press.
*Keywords* – upper ocean, mixed layer, and SST

Sarmiento, J.L., Fasham, M.J.R., Siegenthaler, U., Najjar, R., Toggweiler, J.R. 1989. Models of chemical cycling in the oceans: progress report II. *Ocean Tracers Laboratory Technical Report No. 6.*

*Keywords* – upper ocean, mixed layer, new production, surface ocean bio model, OGCM, DOC, commented, and DOE
*Description* – Uses the model of Toggweiler (JGR 94 (C6), 8217-8265, '89). Also describes the nutrient-restoring model used to argue that DOC provides an invisible nitrogen pool that is advecting around.

Schopf, P.S., Cane, M.A. 1983. On equatorial dynamics, mixed layer physics, and sea surface temperatures. *J. Phys. Ocean.*, **13**, 917-935.
*Keywords* – upper ocean, equatorial ocean, mixed layer, El Nino, coupled A-O, SST, and commented
*Description* – Use bulk mixed layer physics to do ENSO stuff

Spitzer, W.S., Jenkins, W.J. 1989. Rates of vertical mixing, gas exchange, and new production: estimates from seasonal gas cycles in the upper ocean near Bermuda. *J. Mar. Res.*, **47**, 169-196.
*Keywords* – upper ocean, mixed layer, 1D, thermocline ventilation, new production, dissolved oxygen, gas exchange, commented, thermocline, diapycnal mixing, and DOE
*Description* – He gets a vertical turbulent diffusivity of about 1E-4 m2/s, based on the temperature history and the argon data. Gets new production rates of about 4-6 mol O2/m2y (that's about 50g C/m2y, consistent with Jenkins and Goldman). Also estimates rates of air injection and of gas exchange.

Stevenson, J.W. 1979. On the effect of dissipation on seasonal thermocline models. *J. Phys. Ocean.*, **9**, 57-64.
*Keywords* – upper ocean, mixed layer, 1D, bulk model, wind stress scaling, model comparison, dissipation, commented, and DOE
*Description* – Extensive review of the issue of dissipation in the wind-driven bulk mixed layer models. Some of them mix all the way to the bottom, eventually.

Stevenson, J.W. 1983. The seasonal variation of the surface mixed-layer response to the vertical motions of linear rossby waves. *J. Phys. Ocean.*.
*Keywords* – abstract only, upper ocean, mixed layer, and Rossby waves

Tabata, S. 1961. Temporal changes of salinity, temperature, and dissolved oxygen content of the water at station "P" in the Northeast Pacific Ocean, and some of their determining factors. *J. Fish. Res. Bd. Canada*, **18(6)**, 1073-1124.
*Keywords* – upper ocean, mixed layer, 1D, and data

Tabata, S., Boston, N.E.J., Boyce, F.M. 1965. The relation between wind speed and summer isothermal surface layer of water ot ocean station P in the Eastern Subarctic Pacific Ocean. *J. Geophys. Res.*, **70**, 3867-3878.
*Keywords* – upper ocean, mixed layer, 1D, and data

Therry, G., Lacarrere, P. 1983. Improving the eddy kinetic energy model for planetary boundary layer description. *Boundary-Layer Meteorology*, **25**, 63-88.
*Keywords* – upper ocean, mixed layer, 1D, turbulence closure, commented, and DOE

*Description* – Compared by P. Martin to other types of models. Very similar to Mellor's but they come out with slightly different values for the critical Ri number, on which the response of the models depend.

Thomas, A.C., Strub, P.T. 1989. Large-scale patterns of phytoplankton pigment distribution during the spring transition along the west coast of North America. (manuscript).
*Keywords* – upper ocean, new production, wind forcing, and mixed layer

Thomas, K.J.H. 1989. Vertical circulation revealed by diurnal heating of the upper ocean in late winter, part II: modeling. *J. Phys. Ocean.*, **19**, 279.
*Keywords* – upper ocean, convective mixing, and mixed layer, 1D

Venrick, E.L., McGowan, J.A., Cayan, D.R., Hayward, T.L. 1987. Climate and Chlorophyll a: long-term trends in the central North Pacific Ocean. *Science*, **238**, 70-72.
*Keywords* – upper ocean, mixed layer, new production, and wind forcing
*Description* – Reports that chlorophyll concentrations in the North Pacific have increased over the last 20 years. Correlates that with in increase in winter winds and a decrease in SST.

Woods, J.D. 1980. Diurnal and seasonal variation of convection in the wind-mixed layer of the ocean. *Quarterly J. Royal Met. Soc.*, **106**, 379-394.
*Keywords* – upper ocean, mixed layer, 1D, diurnal cycle, seasonal cycle, convective mixing, and commented
*Description* – He says that wind is only important for mixing during the day, and convection only at night. Modeling this requires a diurnal timestep, but he presents a parameterization which does this with longer time stepping, for climate models.

Woods, J.D., Barkmann, W. 1986. The response of the upper ocean to solar heating. I: The mixed layer. *Quart. J. Roy. Met. Soc.*, **112**, 1-42.
*Keywords* – upper ocean, mixed layer, 1D, optics, commented, and DOE
*Description* – 1.5 deg K error in SST results from inadequate resolution of diurnal cycle (relative to resolved model, not relative to data). Also, 1 deg K error from +- 1 Jerlov scale unit in turbidity, about the uncertainty (see page 20).

Woods, J.D., Barkmann, W. 1986. A lagrangial mixed layer model of Atlantic 18C water formation. *Nature*, **319**, 574-576.
*Keywords* – upper ocean, mixed layer, 1D, and lagrangian model

Zeman, O., Lumley, J.L. 1976. Modeling buoyancy driven mixed layers. *J. Atl. Sci.*, **33**, 1974-1988.
*Keywords* – upper ocean, mixed layer, 1D, turbulence closure, and commented
*Description* – Cited by P. Martin (tech report) as being criticism of Mellor model's transport of turbulence (as being inadequate).

# Appendix III. Descriptions of some existing 1-D coupled biological-physical models

## A.   Archer PAPA model

David Archer, University of Chicago

A one-dimensional model of temperature, salinity, nutrients, oxygen, carbon, and argon chemistry is used to hindcast the annual cycle of sea surface $pCO_2$ at weathership station Papa in the subarctic Pacific ($50°N$, $145°W$), based on recent biological and chemical measurements made in conjunction with the SUPER program. Heat fluxes are calculated from the meteorological time series data from the Canadian weathership program. The Price et al. (1986) model is used for predicting mixed layer dynamics. The rate of new production in the model is based on sediment trap data (Welschmeyer, unpublished) and a comparison of model oxygen and argon concentrations with the recent data of Emerson et al. (1991). The balances of nutrients and oxygen in the permanent halocline require isopycnal ventilation on a time frame of approximately 10 years; this estimate is consistent with the estimate of VanScoy et al. (1991) based on tritium data from Geosecs and Long Lines programs. The model results are compared with the 5 year time series data presented by Wong et al. (1990). The model appears to capture the mean sea surface $pCO_2$ and the magnitude and timing of the seasonal cycle. The data however contain much greater high frequency variation than the model results, which we believe is caused by patchiness in the horizontal distribution of $NO_3$. The model $pCO_2$ sensitivity to the chemistry of the upwelling water and the rate of biological new production are presented. Although the model simulation of $pCO_2$ is satisfactory, this study illustrates the limitations of modeling the chemistry of the upper ocean in one dimension. The slow currents and horizontally homogeneous sea surface in the subarctic Pacific make Papa one of the best available candidates for modeling in 1-D. In spite of this, a 1-D formulation is inadequate to address the chemistry of the halocline (a crucial lower boundary condition to the mixed layer) and does not constrain the transport of the nutrients by wind-driven currents in the mixed layer. We conclude that further progress in modeling the upper ocean nutrient and carbon cycles will require simulation in three dimensions.

## B. PWPBIO_OPT: A Fully-Coupled One-Dimensional Physical-Bio-Optical Model

John Moisan, Scripps Institution of Oceanography

### 1. Model Description

The model is a one-dimensional (vertical) time-dependent physical-bio-optical model. The physical portion includes the effects of vertical velocity (biological and advective), background vertical diffusion, and Price-Weller-Pinkel mixed-layer dynamics (Price et al., 1986; hereafter PWP). The biological portion of the model consists of a general $N$-component food web which can be easily reconfigured to the specifications required for other mixed-layer bio-optical modeling programs. As an example, the model is currently configured with a nine component food-web that includes silicate, nitrate, ammonium, two phytoplankton size fractions, three zooplankton categories and a detrital pool (Moisan, 1992). Transfers within this food web occur through nutrient uptake by phytoplankton, differential grazing by zooplankton and nutrient recycling. Finally, coupled to the general food web model is a modified version of the subsurface spectral irradiance model of Sathyendranath and Platt (1988).

### 2. Physical Model

The governing equations which are used in this model are the one-dimensional primitive equations:

$$\frac{\partial u}{\partial t} + w\frac{\partial u}{\partial z} - fv - \frac{\partial}{\partial z}\left(K_z\frac{\partial u}{\partial z}\right) = \mathcal{F}_u - \delta u - \frac{1}{\rho}\frac{\partial \tau_x}{\partial z} \tag{1}$$

$$\frac{\partial v}{\partial t} + w\frac{\partial v}{\partial z} + fu - \frac{\partial}{\partial z}\left(K_z\frac{\partial v}{\partial z}\right) = \mathcal{F}_v - \delta v - \frac{1}{\rho}\frac{\partial \tau_y}{\partial z} \tag{2}$$

$$\frac{\partial T}{\partial t} + w\frac{\partial T}{\partial z} - \frac{\partial}{\partial z}\left(K_z\frac{\partial T}{\partial z}\right) = \mathcal{F}_T - \frac{1}{\rho c}\left(\frac{\partial I}{\partial z} + PHAR\right) \tag{3}$$

$$\frac{\partial S}{\partial t} + w\frac{\partial S}{\partial z} - \frac{\partial}{\partial z}\left(K_z\frac{\partial S}{\partial z}\right) = \mathcal{F}_S - \frac{\partial E}{\partial z} \tag{4}$$

where the terms and parameters in equations 1-4 are defined in Table 1.

Equations 1 and 2 express the $u$, $v$ momentum balances, respectively. The time evolution of the temperature, $T(z,t)$, and salinity, $S(z,t)$, fields, which govern the density, $\rho(z,t)$, are given by equations 3 and 4, respectively.

The vertical velocity at the sea surface, the top of the model domain, is set to zero,

$$w(z = 0\ m, t) = 0.$$

The vertical velocity at the bottom of the domain, $z_{max}$, is defined as:

$$w(z = z_{max}, t) = f(t),$$

57

**Table 1.** Definition of Terms in the Primitive Equations For the One-Dimensional Model

| Terms | Definition |
|---|---|
| $u(z,t)$ | horizontal velocity in the x-direction |
| $v(z,t)$ | horizontal velocity in the y-direction |
| $w(z,t)$ | vertical velocity |
| $T(z,t)$ | temperature |
| $S(z,t)$ | salinity |
| $\rho(z,t)$ | density |
| $\tau_x$ | wind stress in the x-direction |
| $\tau_y$ | wind stress in the y-direction |
| $c$ | specific heat of seawater |
| $f$ | Coriolis parameter |
| $g$ | acceleration of gravity |
| $\delta$ | linear drag coefficient |
| $K_z(z)$ | background diffusion term |
| $(\mathcal{F}_u, \mathcal{F}_v, \mathcal{F}_T, \mathcal{F}_S)$ | climatological forcing terms |
| $I(z)$ | subsurface solar irradiance |
| $PHAR(z)$ | photosynthetically absorbed radiation |
| $E(z)$ | evaporation minus precipitation |

where $f(t)$ represents a time-varying or constant vertical velocity. The interior vertical velocities are then obtained by assuming a linear dependence in the vertical between the surface and the bottom of the model domain,

$$\frac{\partial w(z,t)}{\partial z} = \frac{w(z = z_{max}, t) - w(z = 0\ m, t)}{z_{max}}.$$

The interior vertical velocities are then obtained from:

$$w(z,t) = \frac{w(z = z_{max}, t)}{z_{max}} z,$$

where $z$ is the depth. This method assumes a constant horizontal divergence throughout the model domain. Finally, a background vertical diffusion term, $K_z(z)$, is included in the model as a depth-dependent term. By doing this, diffusion can be increased in regions of the domain where wind mixing may not play an important role but mixing due to other processes is known to occur.

## 3. PWP Mixed-Layer Dynamics

The model incorporates PWP mixed-layer dynamics (Price et al., 1986). Vertical mixing occurs in the model in order to meet the following three criteria of the PWP mixing scheme:

1) The first mixing criteria simulates free convective mixing in the water column in order to achieve static stability. This requires that

$$\frac{\partial \rho}{\partial z} \leq 0. \tag{5}$$

2) The second criteria simulates the entrainment of the mixed-layer. Termed mixed-layer stability, this entrainment process is accomplished by a relaxation of the bulk Richardson number

$$R_b = \frac{g \Delta \rho h}{\rho_0 (\Delta V)^2} \geq 0.65. \tag{6}$$

3) Finally, mixing due to the effect of shear flow instability is simulated by a relaxation of a gradient Richardson number

$$R_g = \frac{g \partial \rho / \partial z}{\rho_0 (\partial V / \partial z)^2} \geq 0.25, \tag{7}$$

The forcing of the model is accomplished through the terms in the primitive equations which have been presented earlier.

## 4. Biological Processes

The biological model is a system of $N$ coupled partial differential equations that govern the vertical and time distribution of a non-conservative quantity, and is of the form;

59

$$\frac{\partial B}{\partial t} + (w + w_{biology})\frac{\partial B}{\partial z} - \frac{\partial}{\partial z}\left(K_z\frac{\partial B}{\partial z}\right) = \mathcal{F}_B + S, \tag{8}$$

where $B$ is a non-conservative quantity (one of the $N$ components in the biological model), $w$ is the vertical advective velocity, $w_{biology}$ is the vertical sinking rate of the biological component, $\mathcal{F}_B$ is the climatological forcing term and $S$ is the source or sink term for $B$.

## 5. Optical Model

The bio-optical portion of the model simulates the wavelength-, depth- and time-dependent downwelling irradiance field between 300 and 4000 nm with a spectral resolution as high as 5 nm. Both the direct and diffuse components of spectral irradiance at the sea surface are calculated using a simple, wavelength-dependent, solar irradiance model for direct-normal and diffuse horizontal irradiance (Bird, 1984). The wavelength-dependent attenuation of the subsurface irradiance field, due to sea water, phytoplankton and dissolved organic matter is simulated using a modified version of the Sathyendranath and Platt (1986) subsurface solar irradiance model. The gradient of the flux of the subsurface solar irradiance is incorporated as a depth-dependent energy flux which balances the phytoplankton energy uptake and the thermal energy flux ($\Delta T$) into the water column.

## 6. Model Implementation

A spectral collocation, method was used to solve the system of equations that define the physical-bio-optical model. The model uses a leap-frog timestepping scheme with occasional leap-frog trapazoidal or Adams-Bashforth timestep in order to remove the effect of timesplitting from the solution. This provides consistency with the approach used to obtain solutions to the 3-D circulation model (Haidvogel et al., 1991$b$) that provided input to the current configuration of this model (Moisan, 1993). A more complete description of this spectral technique can be found in Haidvogel et al. (1991$a$).

## 7. References

Bird, R. E., A simple, solar spectral model for direct-normal and diffuse horizontal irradiance, *Solar Energy*, *32*, 461-471, 1984.

Haidvogel, D. B., A. Beckmann and K. S. Hedström, Dynamical simulations of filament formation and evolution in the Coastal Transition Zone, *J. Geophys. Res.*, *96*, 15,017-15,040, 1991a.

Haidvogel, D. B., J. Wilkin and R. E. Young, A semi-spectral primitive equation ocean circulation model using vertical sigma and orthogonal curvilinear coordinates, *J. Comp. Phys.*, *94*, 151-185, 1991b.

Moisan, J., Modeling nutrient and plankton processes in the California Coastal Transition Zone, Ph. D. thesis, 214 pp., Old Dominion University, Norfolk, Virginia, 1993.

Moisan, J., A vertical, time-dependent bio-optical model, in *Primary Productivity and Biogeochemical Cycles in the Sea*, edited by P. G. Falkowski and A. D. Woodhead, Plenum Press, New York, 522-523, 1992.

Price, J., R. Weller and R. Pinkel, Diurnal cycling: Observations and models of the upper ocean response to diurnal heating, cooling, and wind mixing, *J. Geophys. Res.*, *91*, 8411-8427, 1986.

Sathyendranath, S., and T. Platt, The spectral irradiance field at the surface and in the interior of the ocean: A model for applications in oceanography and remote sensing, *J. Geophys. Res.*, *95*, 9270-9280, 1988.

## C.  Hood/Olson PWP+NPZD Coupled Model

Raleigh Hood and Donald Olson, RSMAS, University of Miami

We are currently working with a coupled $PWP/NPZD$ biophysical model (Price, Weller, and Pinkel (1986) mixed layer model driving a nitrogen ($N$), phytoplankton ($P$), zooplankton ($Z$) and detritus ($D$) ecosystem model).

The four compartment biological model was developed by Glen Flierl, Don Olson and Cabell Davis (unpublished). The basic set of equations are:

$$\frac{\partial N}{\partial t} = (\zeta - \gamma)gPZ + \delta dZ + eD - uIPN$$

$$\frac{\partial P}{\partial t} = uIPN - gPZ - sP$$

$$\frac{\partial Z}{\partial t} = \gamma gPZ - dZ$$

$$\frac{\partial D}{\partial t} = (1 - \zeta)gPZ + (1 - \delta)dZ + sP - eD$$

The terms are defined in the accompanying table along with a schematic box diagram of the model showing the pathways and the directions of flows of nitrogen between the four compartments.

In this version the phytoplankton growth rate is linearly dependent upon both light and nutrients, zooplankton grazing rate is linearly dependent upon phytoplankton biomass, and the closure is the simple $Z$ form. As such, equilibrium solutions are easily obtained. During the URIP workshop we incorporated Michaelis-Menten saturation functions for production versus irradiance and production versus nitrogen concentration, and a modified Ivlev zooplankton grazing function (see Physics Working Group Report, PWP+NPZD, this volume). We also plan to use a $Z^2$ closure in future simulations.

The essential difference between $NPZD$ and simpler $NPZ$ models (e.g. Flierl and Davis, 1993) is, obviously, the additional $D$ compartment. This box can be considered a simple "microbial loop", where the detritus remineralization rate ($e$) is the rate at which bacteria convert detritus-nitrogen to dissolved-nitrogen. Thus in the $NPZD$ model bacterial processes are explicitly represented. Also, the $D$ compartment allows more realistic simulation of sinking.

Our $NPZD$ biological model runs as a subroutine in a modified version of $PWP$. Nitrogen concentrations in each compartment are passively mixed (and optionally diffused) by the PWP mixing (and diffusion) subroutines. As with temperature and salt, the mixing is done to satisfy the stability criterion in the physical model (See Price et al., 1986). Our version of $PWP$ has been modified as follows:
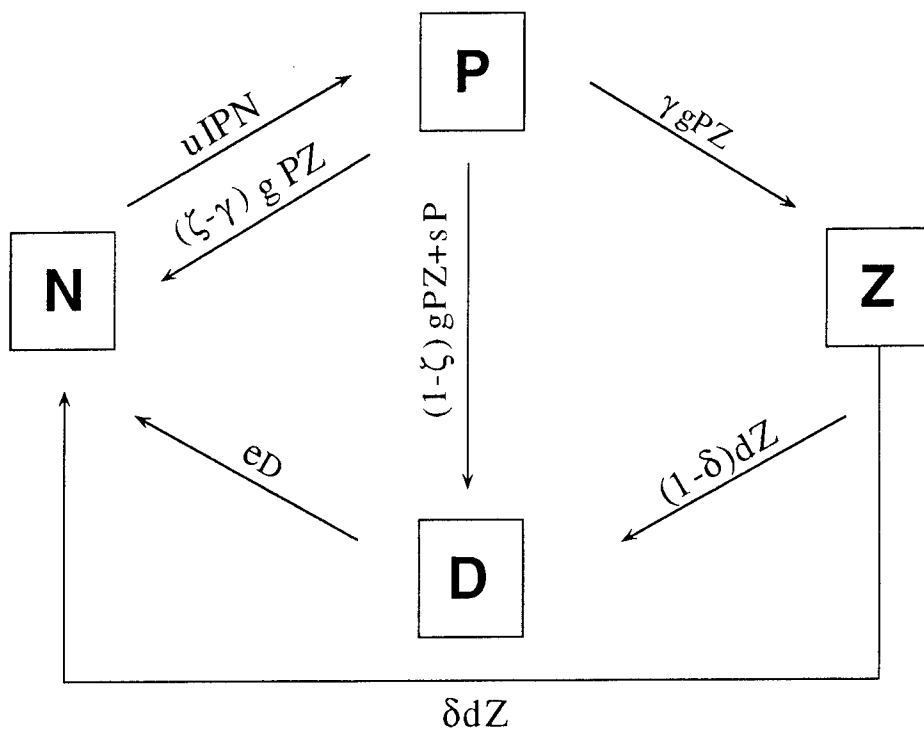
- The original diffusion subroutine in PWP (forward time centered space or FTCS) has been replaced with a Crank-Nicholson scheme (Press et al., 1986), and the bottom boundary condition has been modified to allow upward diffusion of dissolved nitrogen.
- An additional subroutine, which is analogous to the Crank-Nicholson diffusion subroutine, has been added that allows detrital sinking and loss at the bottom boundary.
- The dual wavelength light attenuation/absorption model (Paulson and Simpson, 1977) has been modified to take into account the effects of phytoplankton absorption. The phytoplankton absorb only blue light according to a constant nitrogen-specific diffuse attenuation coefficient (equivalent to a $K_c = 0.014$ $m^2$ $mgChla^{-1}$; Kirk, 1983). It is assumed that only 10% of the light absorbed by phytoplankton is converted to photochemical energy, and that the remaining 90% ends up as heat.
- We have incorporated empirical surface forcing formulae from Bleck et al. (1989) that provide idealized annual cycles in insolation, heat loss (latent, sensible and back radiation) and wind stress for the North Atlantic ocean as functions of latitude.

**Coupled Indian Ocean Model:**

In collaboration with Jay McCreary at NOVA University we have also installed an $NPZD$ ecosystem model in a 2.5-layer Indian Ocean circulation model (the latter is described in McCreary et al., 1993). A surface mixed layer embedded in the upper layer of the physical model determines the light (mixed layer depth) and nutrient (entrainment and detrainment) environments for the biological model. The four biological compartments are advected horizontally and sinking is simulated in the vertical.

**References:**

Bleck, R., H. P. Hanson, D. Hu, and E. B. Kraus, 1989: Mixed layer–thermocline interaction in a three-dimensional isopycnic coordinate model, *J. Phys. Oceanogr.*, **19**: 1417-1439.

Flierl, G. R. and C. S. Davis, 1993: Biological effects of Gulf Stream meandering, *J. Mar. Res.*, in press.

Kirk, J. T. O., 1983: *Light and Photosynthesis in Aquatic Ecosystems.* Cambridge University Press, Cambridge, p. 273.

McCreary, J. P. Jr., P. K. Kundu, and R. L. Molinari, 1993: A numerical investigation of dynamics, thermodynamics and mixed-layer processes in the Indian Ocean. *Prog. Oceanogr.*, in press.

Paulson, C. A., and Simpson, 1977: Irradiance measurements in the upper ocean, *J. Phys. Oceanogr.*, **7**: 952-956

Press, W. H., B. P. Flannery, S. A. Teukolsky, and W. T. Vetterling, 1986: *Numerical Recipes: The Art of Scientific Computing.* Cambridge University Press, Cambridge, p. 638.

Price, J. F., R. A. Weller, and R. Pinkel, 1986: Diurnal cycling: Observations and models of the upper ocean response to diurnal heating, cooling, and wind mixing, *J. Geophys. Res.*, **91**: 8411-8427.

$$\text{uIPN} \quad P \quad \gamma gPZ$$

$$(\zeta-\gamma)\,g\,PZ$$

$$N \qquad (1-\zeta)\,gPZ+sP \qquad Z$$

$$eD \qquad (1-\delta)dZ$$

$$D$$

$$\delta dZ$$

N-P-Z-D Model Symbols and Units:

| Description | Symbol | Units |
| --- | --- | --- |
| Dissolved nitrogen | $N$ | $\mu M$ |
| Phytoplankton nitrogen | $P$ | $\mu M$ |
| Zooplankton nitrogen | $Z$ | $\mu M$ |
| Detritus nitrogen | $D$ | $\mu M$ |
| Light intensity | $I$ | dimensionless |
| Phytoplankton growth rate | $u$ | $s^{-1}\mu M^{-1}$ |
| Zooplankton Grazing rate | $g$ | $s^{-1}\mu M^{-1}$ |
| Zooplankton Death rate | $d$ | $s^{-1}$ |
| Detritus remineralization rate | $e$ | $s^{-1}$ |
| Phytoplankton scenscence rate | $s$ | $s^{-1}$ |
| Growth efficiency for Z | $\gamma$ | dimensionless |
| Assimililation efficiency for Z | $\zeta$ | dimensionless |
| Assimilation efficiency for higher trophic levels† | $\delta$ | dimensionless |

†growth efficiency for higher trophic levels set at zero

University of California, San Diego
SIO Library 0175C (TRC)
9500 Gilman Drive
La Jolla, CA 92093-0175

Hancock Library of Biology & Oceanography
Alan Hancock Laboratory
University of Southern California
University Park
Los Angeles, CA 90089-0371

Gifts & Exchanges
Library
Bedford Institute of Oceanography
P.O. Box 1006
Dartmouth, NS, B2Y 4A2, CANADA

Commander
International Ice Patrol
1082 Shennecossett Road
Groton, CT 06340-6095

NOAA/EDIS Miami Library Center
4301 Rickenbacker Causeway
Miami, FL 33149

Library
Skidaway Institute of Oceanography
10 Ocean Science Circle
Savannah, GA 31411

Institute of Geophysics
University of Hawaii
Library Room 252
2525 Correa Road
Honolulu, HI 96822

Marine Resources Information Center
Building E38-320
MIT
Cambridge, MA 02139

Library
Lamont-Doherty Geological Observatory
Columbia University
Palisades, NY 10964

Library
Serials Department
Oregon State University
Corvallis, OR 97331

Pell Marine Science Library
University of Rhode Island
Narragansett Bay Campus
Narragansett, RI 02882

Working Collection
Texas A&M University
Dept. of Oceanography
College Station, TX 77843

Fisheries-Oceanography Library
151 Oceanography Teaching Bldg.
University of Washington
Seattle, WA 98195

Library
R.S.M.A.S.
University of Miami
4600 Rickenbacker Causeway
Miami, FL 33149

Maury Oceanographic Library
Naval Oceanographic Office
Building 1003 South
1002 Balch Blvd.
Stennis Space Center, MS 39522-5001

Library
Institute of Ocean Sciences
P.O. Box 6000
Sidney, B.C. V8L 4B2
CANADA

Library
Institute of Oceanographic Sciences
Deacon Laboratory
Wormley, Godalming
Surrey GU8 5UB
UNITED KINGDOM

The Librarian
CSIRO Marine Laboratories
G.P.O. Box 1538
Hobart, Tasmania
AUSTRALIA 7001

Library
Proudman Oceanographic Laboratory
Bidston Observatory
Birkenhead
Merseyside L43 7 RA
UNITED KINGDOM

IFREMER
Centre de Brest
Service Documentation - Publications
BP 70 29280 PLOUZANE
FRANCE

| REPORT DOCUMENTATION PAGE | 1. REPORT NO. WHOI-94-32 | 2. | 3. Recipient's Accession No. |
|---|---|---|---|

| 4. Title and Subtitle Biological/Physical Modeling of Upper Ocean Processes | 5. Report Date September 1994 |
|---|---|
| | 6. |

| 7. Author(s)   Cabell S. Davis and John H. Steele | 8. Performing Organization Rept. No. WHOI-94-32 |
|---|---|

| 9. Performing Organization Name and Address  Woods Hole Oceanographic Institution Woods Hole, Massachusetts 02543 | 10. Project/Task/Work Unit No. |
|---|---|
| | 11. Contract(C) or Grant(G) No. (C)   N00014-92-J-1527 (G) |

| 12. Sponsoring Organization Name and Address  Office of Naval Research | 13. Type of Report & Period Covered Technical Report |
|---|---|
| | 14. |

**15. Supplementary Notes**

**16. Abstract (Limit: 200 words)**

To enhace collaboration between researchers who model upper ocean biological/physical processes, a workshop was held at WHOI on June 7-12, 1993. The workshop was part of our on-going URIP project entitled "Modeling Biological-Physical Interactions: A Population Biological Approach" sponsored by ONR (Grant N00014-92-J-1527). The two principal goals of the workshop were to: 1) identify critical problems related to mixed-layer biological-physical models, and 2) develop approaches for solving these problems. The workshop was organized into two parts to address these goals. The first part, held over the first day and a half, included three overview presentations given in plenary followed by working groups, organized along disciplinary lines, to identify critical issues. The second part of the workshop consisted of working groups, organized across disciplines, using "hands-on" modeling to address critical aspects of coupled biological-physical models. Several coupled models were presented and/or developed at the workshop addressing specific aspects of both the biological and physical dynamics. These aspects included the different mixed-layer formulations, a structured grazer population model, and an allometric food-web model including microbial-loop dynamics.

**17. Document Analysis    a. Descriptors**

Biological/Physical Modeling
Upper Ocean
Mixed-Layer

**b. Identifiers/Open-Ended Terms**

**c. COSATI Field/Group**

| 18. Availability Statement  Approved for public release; distribution unlimited. | 19. Security Class (This Report) UNCLASSIFIED | 21. No. of Pages 70 |
|---|---|---|
| | 20. Security Class (This Page) | 22. Price |